

Geochemical characterization of marker tephra layers from major Holocene eruptions, Kamchatka Peninsula, Russia

Philip R. Kyle^{a*}, Vera V. Ponomareva^b and Rachele Rourke Schluep^a

^aDepartment of Earth and Environmental Science, New Mexico Institute of Mining and Technology, Socorro, NM, USA; ^bInstitute of Volcanology and Seismology, Petropavlovsk-Kamchatsky, Russia

(Accepted 26 October 2009)

Kamchatka Peninsula is one of the most active volcanic regions in the world. Many Holocene explosive eruptions have resulted in widespread dispersal of tephra-fall deposits. The largest layers have been mapped and dated by the ¹⁴C method. The tephra provide valuable stratigraphic markers that constrain the age of many geological events (e.g. volcanic eruptions, palaeotsunamis, faulting, and so on). This is the first systematic attempt to use electron microprobe (EMP) analyses of glass to characterize individual tephra deposits in Kamchatka. Eighty-nine glass samples erupted from 11 volcanoes, representing 27 well-identified Holocene key-marker tephra layers, were analysed. The glass is rhyolitic in 21 tephra, dacitic in two, and multimodal in three. Two tephra are mixed with glass compositions ranging from andesite/dacite to rhyolite. Tephra from the 11 eruptive centres are distinguished by their glass K₂O, CaO, and FeO contents. In some cases, individual tephra from volcanoes with multiple eruptions cannot be differentiated. Trace element compositions of 64 representative bulk tephra samples erupted from 10 volcanoes were analysed by instrumental neutron activation analysis (INAA) as a pilot study to further refine the geochemical characteristics; tephra from these volcanoes can be characterized using Cr and Th contents and La/Yb ratios.

Unidentified tephra collected at the islands of Karaginsky (3), Bering (11), and Attu (5) as well as Uka Bay (1) were correlated to known eruptions. Glass compositions and trace element data from bulk tephra samples show that the Karaginsky Island and Uka Bay tephra were all erupted from the Shiveluch volcano. The 11 Bering Island tephra are correlated to Kamchatka eruptions. Five tephra from Attu Island in the Aleutians are tentatively correlated with eruptions from the Avachinsky and Shiveluch volcanoes.

Keywords: tephra; Kamchatka; tephrochronology; volcanic glass; microprobe; INAA

Introduction

Tephrochronology is the study of volcanic ash (tephra) for the purpose of correlating and dating volcanic and other geologic events (Shane 2000; Alloway *et al.* 2007). Volcanic ash from large explosive eruptions is dispersed instantaneously and often over vast areas, making them very useful marker horizons for dating a variety of geologic events (Knox 1993). In addition to the geochronological value, tephra beds are a major source of data on the eruption frequency and geochemistry of explosive volcanoes. In the proximal setting,

*Corresponding author. Email: kyle@nmt.edu

the eruptive source of a tephra can often be identified using lithology, stratigraphic position, and mineralogy. Farther from the source, these features become less diagnostic as units become thinner and the denser minerals have settled from the ash plume, requiring the need for geochemical fingerprinting for correlations (Shane 2000). Geochemical analysis of volcanic glass, often referred to as fingerprinting, is widely used in stratigraphic correlation of tephra. Single-grain analytical techniques such as electron microprobe (EMP) analyses are commonly required to assess the compositional homogeneity of the tephra and to avoid xenolithic and detrital contaminants.

Kamchatka is one of the most active areas of volcanism on earth. Thirty-seven large volcanic centres and hundreds of monogenetic vents have been active during the Holocene (Ponomareva *et al.* 2007a). Many eruptions were highly explosive and formed extensive tephra-fall layers. Holocene ash layers preserved in peats and soils make up the soil-pyroclastic cover that blankets much of the Kamchatka Peninsula, providing a continuous record of the explosive volcanic eruptions during the Holocene (Braitseva *et al.* 1997). Older Pleistocene tephra have mostly been removed during glaciation and occur only in isolated outcrops.

In this study, we characterized the geochemical compositions of Holocene marker tephra to establish their geochemical signature. The signature can be used to identify the tephra that make excellent stratigraphic markers for dating and correlating various deposits and landforms. The tephra were erupted from 11 of the most explosive Holocene volcanoes in Kamchatka (see supplementary Table S1, available with the online version of this article at <http://www.informaworld.com/tigr>). The tephra were identified using stratigraphic correlations, mineralogical and geochemical characteristics of bulk samples, ^{14}C dating, and ash dispersal axes (Braitseva *et al.* 1995, 1997, 1998; Pevzner *et al.* 1998; Bazanova *et al.* 2003, 2005; Ponomareva *et al.* 2004, 2007b). Further identification of the tephra sources was also made possible through detailed mapping of Holocene eruptive centres (Melekestsev *et al.* 1974). Glass chemistry is the most important aspect of the study because glass has the lowest density and is often the most abundant fraction of the tephra. Glass occurs at all locations along the dispersal axes of the eruptions. Unidentified tephra samples from the islands of Karaginsky (3), Bering (11), and Attu (5) and Uka Bay (1) were analysed to determine their eruptive source. As a pilot study, instrumental neutron activation analyses (INAA) were made of bulk samples of 63 tephra representing 19 eruptions from 10 volcanic centres. Bulk samples of the unidentified tephra (except Attu Island) were also analysed by INAA.

Eruptive history of Holocene volcanoes in Kamchatka

Holocene eruptions in Kamchatka have occurred from three main zones: the Eastern Volcanic Front, the Central Kamchatka Depression, and the Sredinny Range (Figure 1). Most of the active Holocene volcanoes are in the Eastern Volcanic Front, which extends along the eastern coast from the Kizimen volcano in the N to the southern end of the Kamchatka Peninsula. The highest magma production rates for volcanoes in Kamchatka occur in the Central Kamchatka Depression.

Large explosive eruptions ($>1\text{ km}^3$ of tephra) have occurred throughout Kamchatka. Eruptions were associated with collapse calderas (Karymsky, three calderas on Ksudach volcanic massif, and Kurile Lake caldera), large individual craters (Baranii Amphitheater, Khodutkinsky, and Chasha craters), and large volcanoes (Shiveluch, Bezymianny, Kizimen, Khangar, Avachinsky, Stübel Cone within the last caldera at Ksudach, and Iliinsky). Most of the large tephra have bulk compositions ranging from andesite to rhyolite in composition.

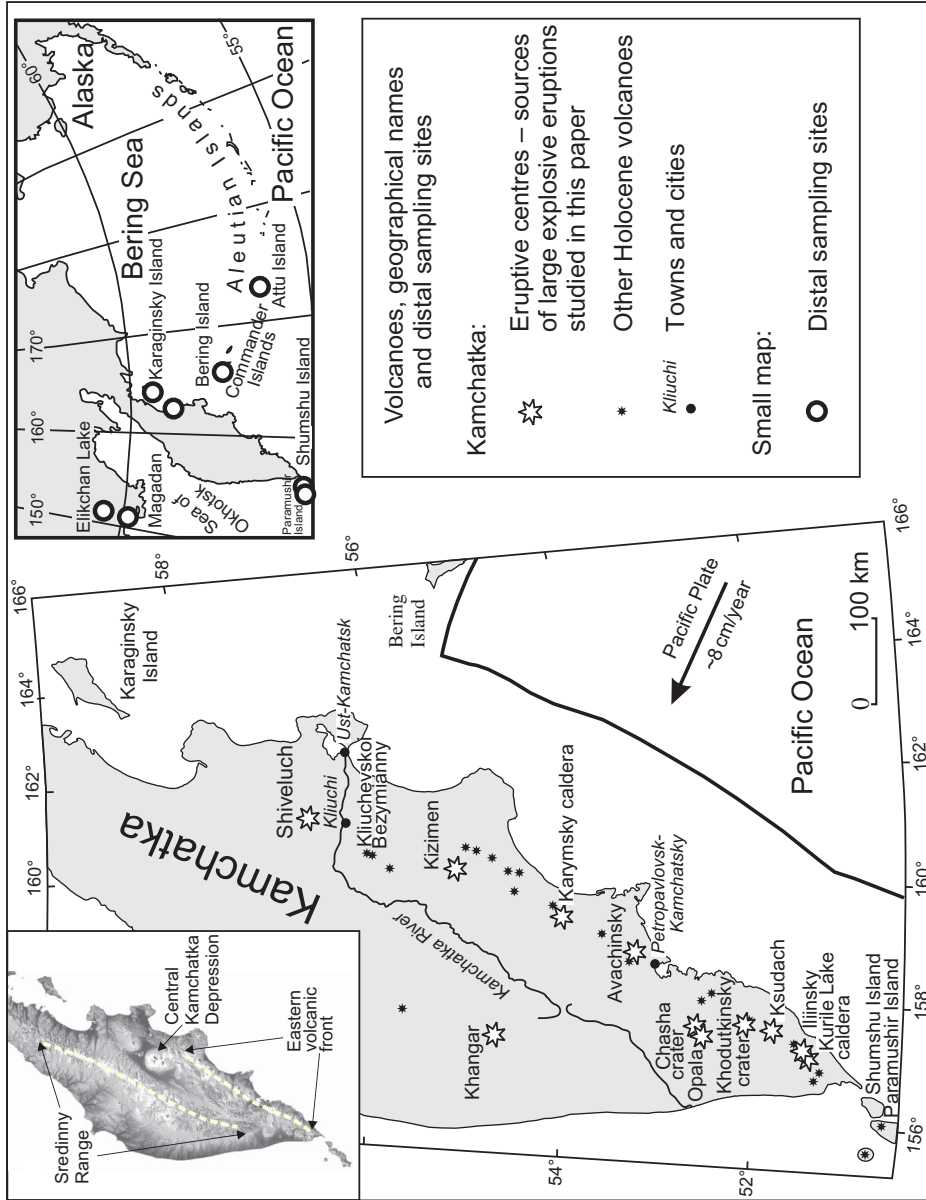


Figure 1. Location map of the Kamchatka Peninsula showing the 11 eruptive centres, which were the source of the tephra examined in this study, and distal sampling sites.

The only large mafic (basaltic andesite) tephra was erupted from the Avachinsky volcano (Bazanova *et al.* 2003).

The age, distribution, and physical characteristics of the largest Holocene key-marker tephra layers erupted from nine volcanic centres have been described by Braitseva *et al.* (1995, 1997). Twenty-seven of these Holocene key-marker tephra layers are examined here. The following section describes the individual volcanoes that erupted the 27 tephra examined, and new isopach maps are presented. The abbreviations and shorthand terminology of the eruptions follow Braitseva *et al.* (1997).

Shiveluch volcano (SH₁₉₆₄, SH₁₈₅₄, SH₁, SH₂, SH₃, SH₁₄₅₀, SH₁₆₀₀, SH₅, SH₂₈₀₀, SH₃₅₀₀, SH_{dv}, SH₄₇₀₀, SH₅₆₀₀)

Shiveluch is a composite volcano at the N end of the Central Kamchatka Depression and currently is the northernmost active volcano in Kamchatka (Figure 1). The Holocene Young Shiveluch eruptive centre is nested in a 9 km-wide sector collapse crater cut into the late Pleistocene Old Shiveluch stratovolcano. Young Shiveluch has an average eruptive frequency of 100–200 years and is one of the most active and prolific in producing marker tephra layers. The last major eruption occurred in 1964 followed by dome growth and accompanying minor eruptions that continue today. Plinian eruptions with tephra volumes $\geq 0.6 \text{ km}^3$ (the size of the 1964 eruption) have occurred at least 23 times during the Holocene and were separated by periods of dome growth (Ponomareva *et al.* 2007b).

Most Shiveluch tephra have bulk compositions of medium-K andesite, although two mafic tephra are known (Ponomareva *et al.* 2007b). The andesitic tephra contain plagioclase, hornblende, magnetite, pyroxene, and more rarely olivine (Braitseva *et al.* 1997). Downwind, the andesitic pumice lapilli grade into crystal-rich coarse ash and then to a fine dominantly vitric ash.

The size of the 13 Shiveluch eruptions examined here is not known in great detail (Table S1), but isopach maps (Figure 2) show that most were $>1 \text{ km}^3$. ^{14}C ages (Table S1) for the eruptions are discussed by Ponomareva *et al.* (2007b).

The SH₂ (950 ^{14}C year BP) tephra resulted from one of the most violent Holocene Plinian eruptions of Shiveluch. The eruption produced $\geq 2 \text{ km}^3$ of tephra that spread out in all directions from the volcano (Figure 2A). The isopach maps suggest that the SH₁₄₅₀, SH₂₈₀₀, and SH_{dv} tephra could have reached the Bering Island (Figure 2E, G, and H).

Kizimen volcano

Kizimen volcano is Holocene and located at the junction of the Eastern Volcanic Front and the Central Kamchatka Depression (Figure 1). It has had four cycles (KZI–KZIV) of activity, each 2–3.5 ka long (Melekestsev *et al.* 1995). Eruptive cycle KZII included a large eruption (KZ) at 7550 ^{14}C year BP that produced 4–5 km^3 of medium-K andesite-to-dacite eruptive products (Figure 3A) which contain plagioclase, hornblende, pyroxene, and magnetite (Braitseva *et al.* 1997). Proximal KZ tephra-fall deposit is a bright-yellow pumice lapilli and coarse ash in a matrix of fine ash. The KZ tephra layer was dispersed to the N and E.

Khargar volcano (KHG)

Khargar volcano is located in the Sredinny Range (Figure 1). A large crater (2.5 \times 2 km) at the summit of Khargar volcano formed at 6850 ^{14}C year BP (Bazanova and Pevzner

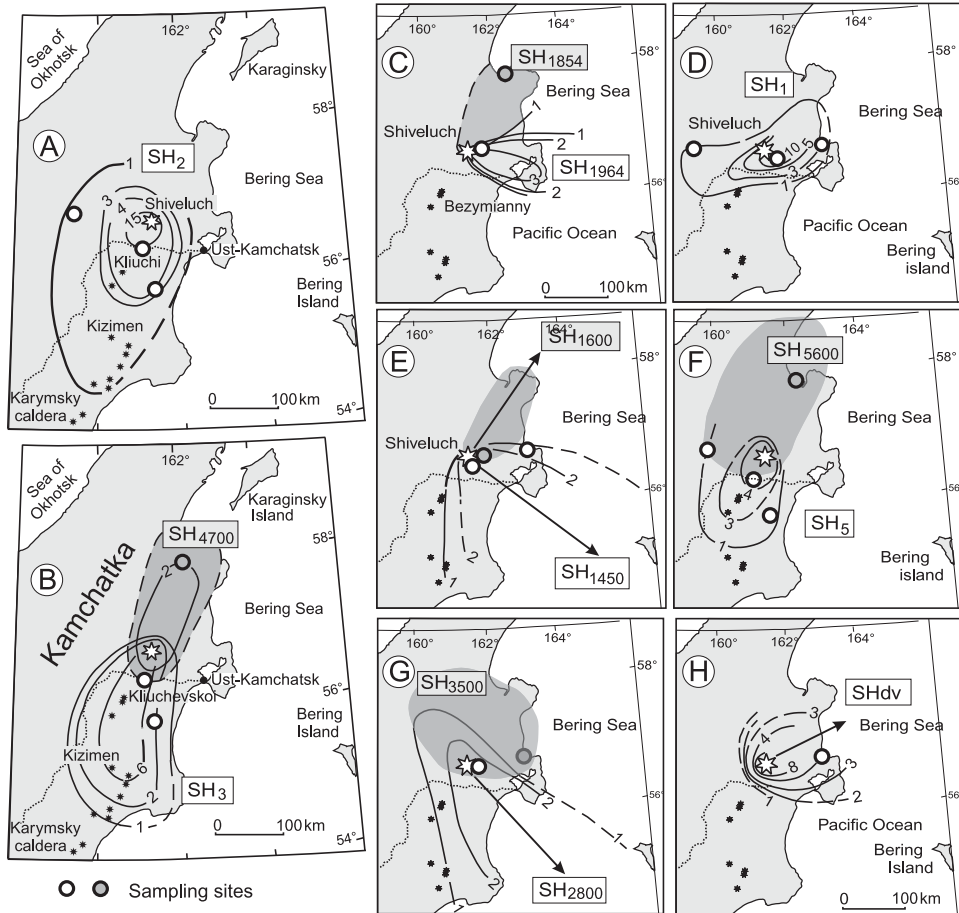


Figure 2. Maps showing the dispersal of tephra erupted from Shiveluch and examined in this study. Isopach are dashed where inferred and thickness is in cm. For tephra layers without isopachs, the area of dispersal is shaded. Sample locations are shown by circles. For codes and ages of the tephra, see Table S1.

2001) producing pyroclastic density current deposits and tephra with a total eruptive volume of 14–16 km³ (Melekestsev *et al.* 1996a). Another eruption of Khangar was reported at ~6600 ¹⁴C year BP (Bazanova and Pevzner 2001). Because the fall deposits of the two eruptions are difficult to map individually, they are combined under the KHG code. KHG tephra was dispersed mainly to the NE (Figure 3B) and is one of the few biotite-bearing Kamchatka tephra, which makes it a valuable marker.

Karymsky volcano (KRM)

Karymsky volcano is one of the most active volcanoes in the Eastern Volcanic Front (Figure 1) and has been in almost continuous eruptions for decades. The stratovolcano sits in a caldera that formed ~7900 ¹⁴C year BP by a major eruption that produced extensive ignimbrites (Braitseva *et al.* 1997) and the KRM tephra-fall deposit. The total eruptive volume was 13–16 km³. KRM pumice is a medium-K rhyodacite. Near source, the KRM

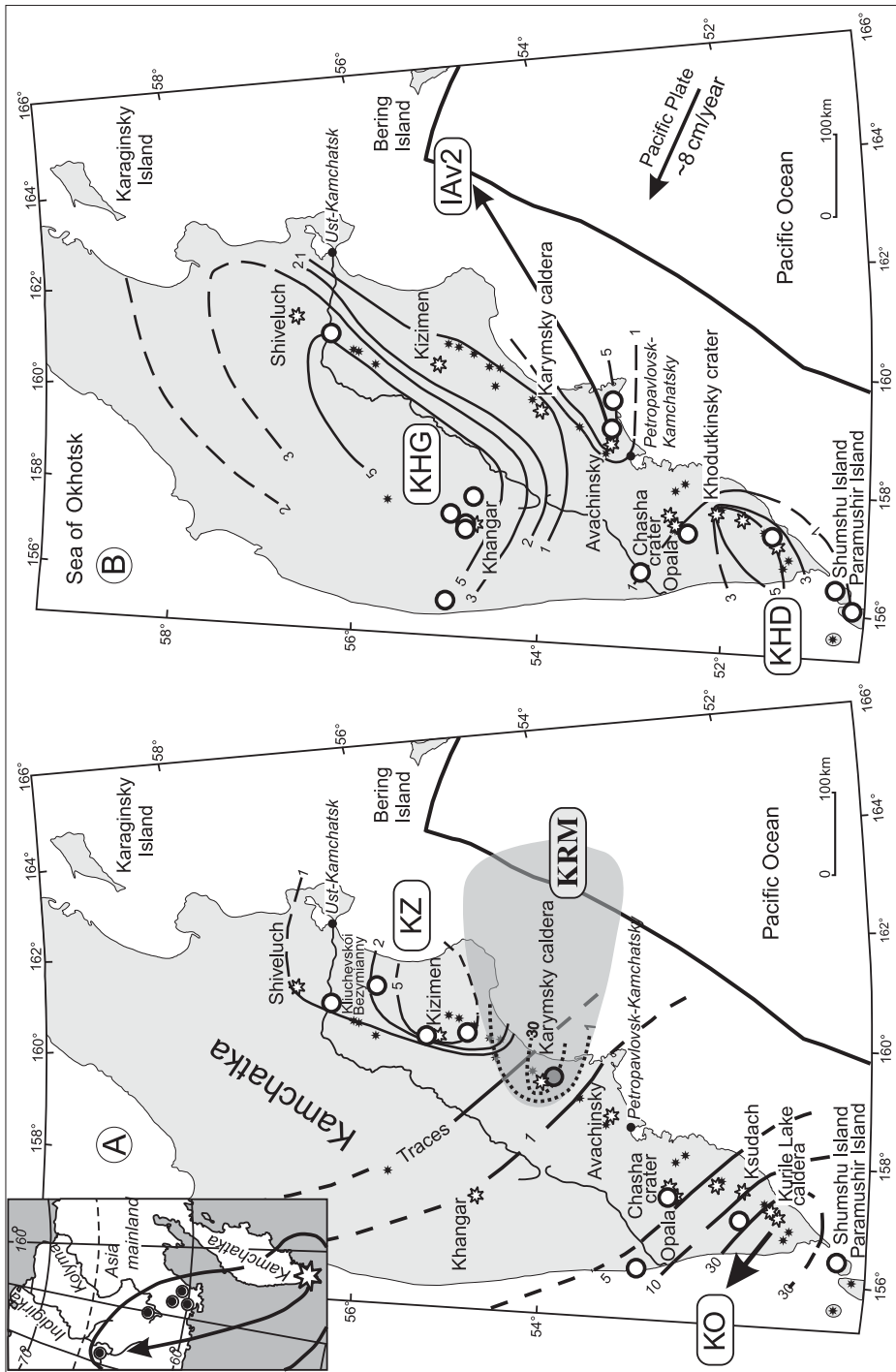


Figure 3. Maps showing the dispersal of marker tephra layers (A) KO, KZ, and KRM and (B) KHG, IAV2, and KHD. Isopach are dashed where inferred and thickness is in cm. For codes and ages of tephra layers, see Table S1. The source volcanoes of the tephra are shown with larger white stars, other volcanoes by small black stars. Sample locations are shown by circles.

fall deposits comprise two pumice bomb and lapilli units separated by surge deposits. The main axis of the tephra fall is to the E with only minor dispersal to the N and S (Braitseva *et al.* 1997) (Figure 3A).

Avachinsky volcano (AV_1 , IAv2)

Avachinsky volcano is 30 km from the city of Petropavlovsk-Kamchatsky (Figure 1) and had a small lava-producing eruption in 1991. The Young Cone of Avachinsky volcano sits in a somma that formed when the summit of a late Pleistocene stratovolcano was destroyed by catastrophic sector collapses 35–40 and 29–30 ka BP (Melekestsev *et al.* 1992).

Two epochs of Holocene eruptions have occurred at Avachinsky (Braitseva *et al.* 1998). The earliest eruptions were mostly andesitic and lasted from 7200 to 3700 ^{14}C year BP. The younger epoch has erupted basaltic andesites. It started 3500 ^{14}C year BP and continues to the present. Over the last 7000 years, Avachinsky volcano has produced at least eight widely dispersed tephra layers, each with a volume $>0.5\text{ km}^3$ (Braitseva *et al.* 1998; Bazanova *et al.* 2003, 2004). Glass compositions of the two largest marker tephra layers (IAv2 and AV_1) are examined here. Bulk INAAs were made of five tephra (AV_1 – AV_5) from Avachinsky to assess the variability in the compositions of the eruptive products over a longer time period.

The IAv2 ($\sim 7150\text{ }^{14}\text{C}$ year BP) Plinian eruption was the largest Holocene eruption of Avachinsky and produced $\geq 8\text{--}10\text{ km}^3$ of tephra that was dispersed to the NE toward Bering Island (Braitseva *et al.* 1998) (Figure 3B). The andesite pyroclastic products (Braitseva *et al.* 1998) contain plagioclase, hornblende, magnetite, and pyroxenes (Braitseva *et al.* 1997). The AV_1 tephra ($\sim 3500\text{ }^{14}\text{C}$ year BP) has a volume $>3.6\text{ km}^3$ and was dispersed to the NE, making it a very important marker for eastern Kamchatka (Braitseva *et al.* 1997) (Figure 4B). It is a product of the Young Cone and has a bulk low-K basaltic andesite composition (Braitseva *et al.* 1997).

Chasha crater (OP_{tr})

Tephra OP_{tr} was produced by an eruption that formed the Chasha Lake crater at Tolmachev lava field about 4600 ^{14}C year BP (Dirksen *et al.* 2002; Zaretskaya *et al.* 2007). The eruption produced $\sim 1\text{ km}^3$ of high-K rhyolitic fall tephra that fell along a NE axis (Figure 4B), making it a good marker ash layer for the regions between Opala volcano and the Avachinsky volcanic group (Braitseva *et al.* 1997).

Opala volcano (OP)

One of the most voluminous Holocene eruptions in Kamchatka formed the Baranii Amphitheater, at the foot of Opala volcano (Figure 1). The eruption dates at $\sim 1500\text{ }^{14}\text{C}$ year BP and produced $9\text{--}10\text{ km}^3$ of biotite-bearing high-K rhyolitic tephra (Braitseva *et al.* 1995). The tephra has been traced to the northern part of Sredinny Range and south to Ksudach volcano (Figure 4A). Distal white fine ash of the OP layer is one of the important marker horizons for eastern and central Kamchatka (Braitseva *et al.* 1997).

Khodutkinsky crater (KHD)

The Khodutkinsky crater eruption ($\sim 2500\text{ }^{14}\text{C}$ year BP) at the base of Khodutka volcano produced $1.0\text{--}1.5\text{ km}^3$ of medium-K hornblende-bearing rhyodacitic tephra. The fall axis

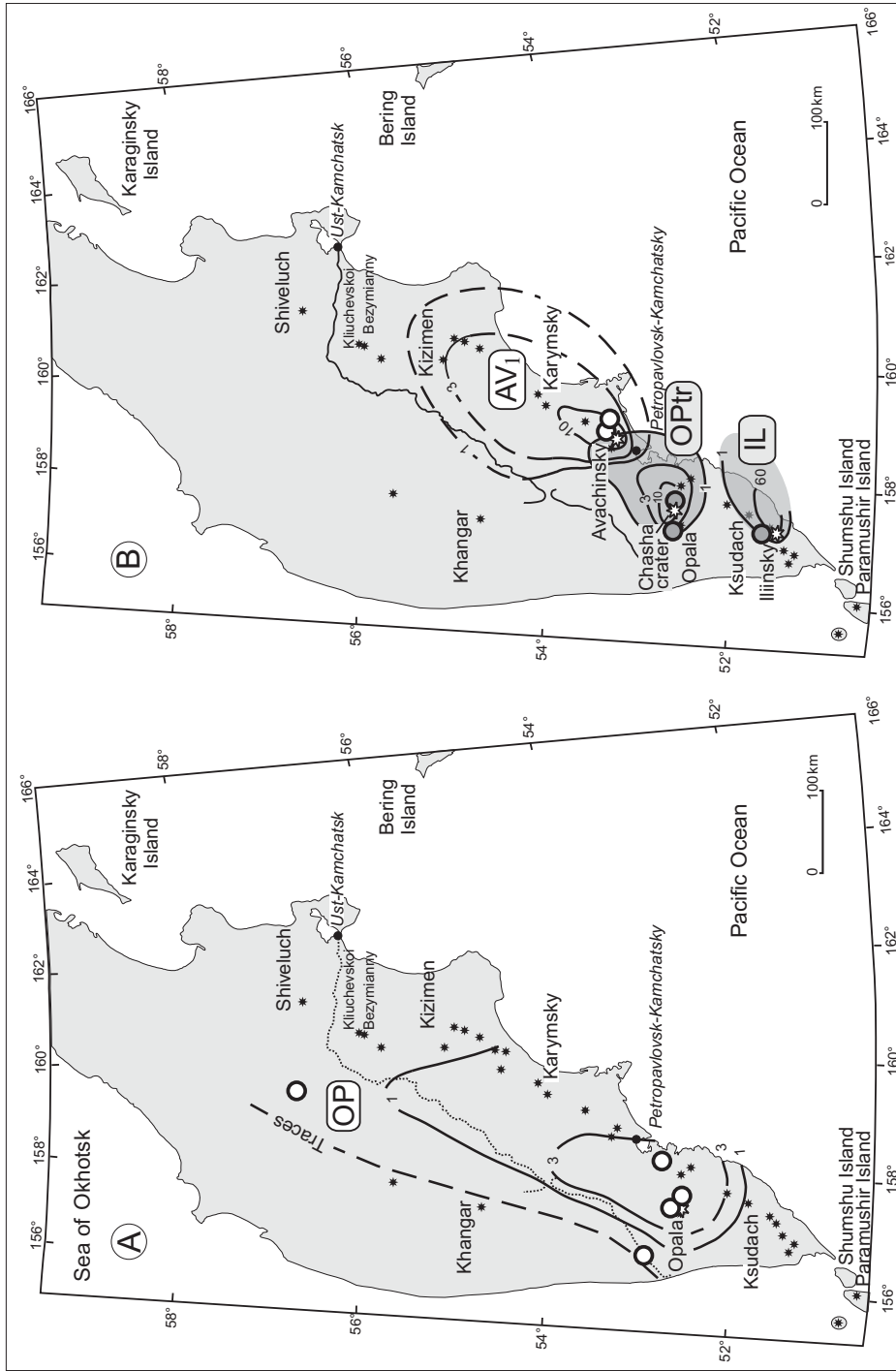


Figure 4. Maps showing the dispersal of marker tephra layers (A) OP and (B) AV₁, OP_{tr}, and IL. Isopach are dashed where inferred and thickness is in cm. For codes and ages of tephra layers, see Table S1. The source volcanoes of the tephra are shown with larger white stars, other volcanoes by small black stars. Sample locations are shown by circles.

was to the SW (Figure 3B), making it an important marker layer for southern Kamchatka and Paramushir Island located S of Kamchatka Peninsula (Zaretskaya *et al.* 2007).

Ksudach volcano (KSht₃, KS₁, KS₂, KS₃)

Six tephra layers formed from the eruptions of Ksudach during the Holocene (Braitseva *et al.* 1997). The four largest tephra are examined here. Ksudach is a huge, gently sloping shield, capped by a complex set of five overlapping calderas (Volynets *et al.* 1999). The two large calderas (I and II) formed in the late Pleistocene and the three smaller ones (III, IV, and V) during the Holocene (Braitseva *et al.* 1995; Melekestsev *et al.* 1996b). Small stratovolcano Stübel Cone is located inside the youngest caldera. The four largest Holocene Ksudach tephra were deposited during eruptions that took place about 8800 (KS₄), 6400 (KS₃), 6000 (KS₂), and 1800 (KS₁) ¹⁴C year BP (Braitseva *et al.* 1997; Volynets *et al.* 1999). The most recent eruption (KSht₃) occurred in 1907 from the Stübel Cone. The tephra deposits of the KS₃ eruption are rhyodacite to dacite, whereas the bulk composition of the KS₂ eruptive products is andesite (Volynets *et al.* 1999). The KS₃ tephra are relatively small (<1 km³) and were dispersed to the W (Figure 5A). The KS₂ eruption volume was 7–8 km³, and tephra were dispersed to the N (Figure 5B) (Braitseva *et al.* 1997). It is one of the most important stratigraphic markers in Kamchatka. Proximal KS₂ tephra is stratified violet-grey thinly banded pumice bombs, whereas the distal tephra is greenish-grey, medium- to fine-grained ash.

The KS₁ eruption was the second largest Holocene eruption in Kamchatka (Braitseva *et al.* 1997) with a volume of 18–19 km³. Proximal erupted products include three fall units of white or yellow pumice topped with a fall unit of grey pumice and separated by density current deposits (Braitseva *et al.* 1996; Andrews *et al.* 2007). A similar sequence has been found in the Kamchatka River valley with yellow ash at the bottom and grey ash at the top (Braitseva *et al.* 1996). The fall tephra can be identified over 1000 km from the source and covered an area of 2–3 million km² (Braitseva *et al.* 1996). Ash fell to the N along the Kamchatka River valley (Figure 5A). The axis shifted eastward during the early eruptions (yellow ash) and westward during the closing phase (grey ash) (Melekestsev *et al.* 1996b). A secondary thickening of the tephra occurs along the Kamchatka River 250 km N of the volcano.

The KSht₃ tephra was dispersed in a northerly direction (Figure 5B) and had a volume of 1.5–2 km³ (Braitseva *et al.* 1997). Proximal KSht₃ tephra consist of two units. The lower part of the tephra is a dark-grey basaltic andesite cinder overlain by thinly banded rhyodacite-to-andesite pumice bombs (Volynets *et al.* 1999).

Iliinsky volcano (IL)

Iliinsky volcano near the S end of the Eastern Volcanic Front (Figure 1) last erupted in 1901. The cone has lava compositions ranging from basalt to dacite, and it has had an extensive eruptive history with many tephra covering southernmost Kamchatka. The ~4850 ¹⁴C year BP IL eruption produced ~1.2–1.4 km³ of tephra that were dispersed in an ENE direction, it is > 60 cm thick at the coast (Figure 4B). Earlier, this tephra was thought to originate from Zheltovsky volcano and was coded ZLT (Braitseva *et al.* 1997). Further field work has identified Iliinsky as the source, and we suggest IL as a code for this tephra (Zaretskaya *et al.* 2007). The IL tephra has proved a valuable layer for dating deposits and landforms along the seashore including palaeotsunami and beach ridges. The tephra is hornblende-bearing dacite to andesite.

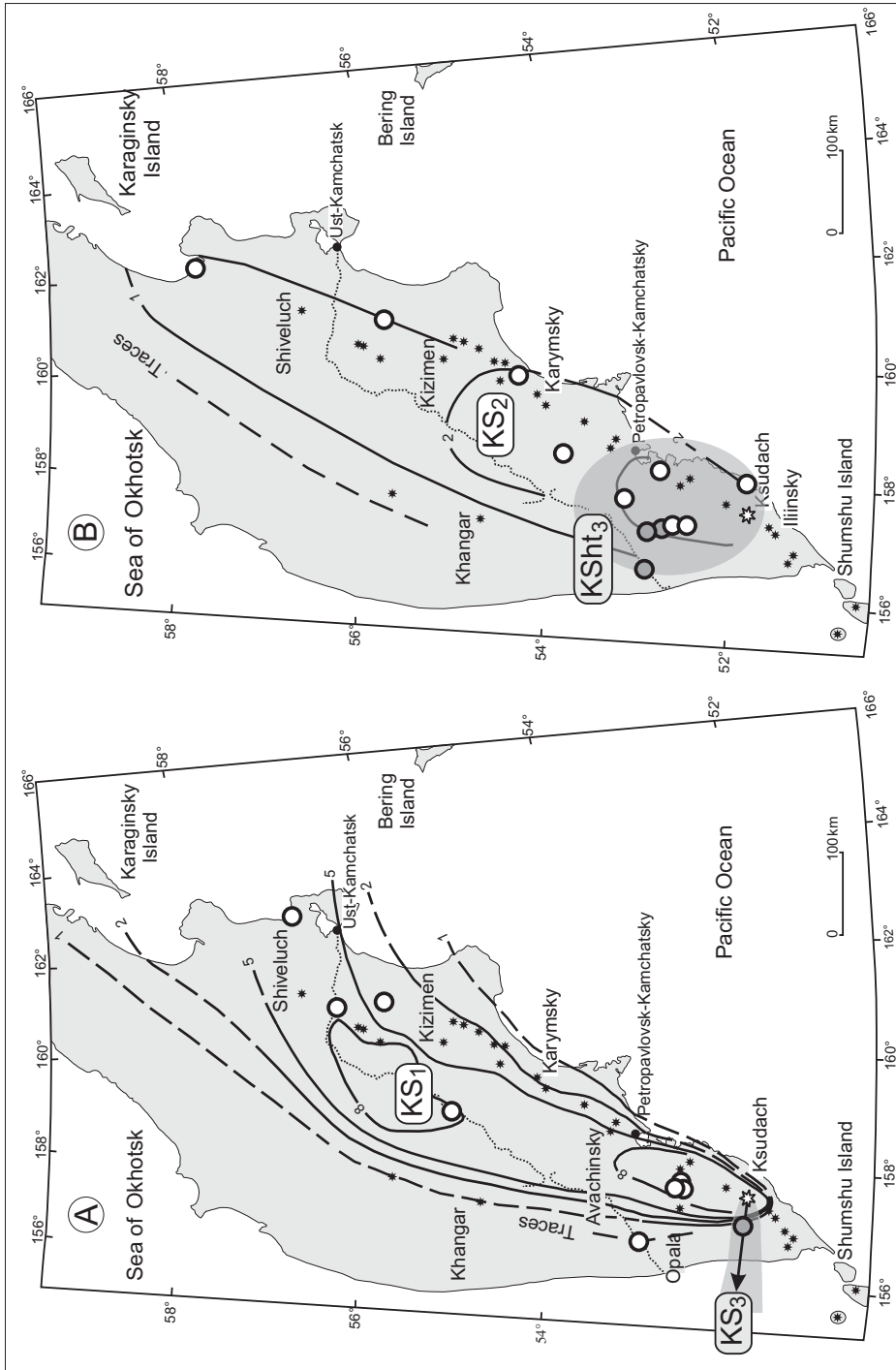


Figure 5. Maps showing the dispersal of marker tephra layers (A) KS₁ and KS₂, and (B) KS₂ and KS₃. Isopach are dashed where inferred and thickness is in cm. For codes and ages of tephra layers, see Table S1. The source volcanoes of the tephra are shown with larger white stars, other volcanoes by small black stars. Sample locations are shown by circles.

Kurile Lake (KO)

Kurile Lake caldera-forming eruption is dated at ~7600 ¹⁴C year BP and was the largest Holocene eruption in Kamchatka (Ponomareva *et al.* 2004). It produced a hornblende-bearing rhyolitic pumice fall and an ignimbrite, which is zoned from rhyolite to basaltic andesite. The total eruptive volume was 140–170 km³. Tephra were dispersed to the NW and have been identified in the Okhotsk Sea cores and on mainland Asia at a distance of ~1700 km from the source (Figures 1 and 3A). It is a valuable marker for a large part of Kamchatka and permits immediate correlation of various Holocene deposits over a vast area of NE Asia.

Analytical methods

Electron microprobe (EMP) analysis

Major element compositions of the glass were measured using a Cameca SX-100 EMP at N.M. Tech, Socorro, NM, USA. An accelerating voltage of 15 kV and beam current of 10 nA were used. Peak counts were 20 seconds for all elements, except Na, Cl, S, and F which were counted for 40, 40, 60, and 100 seconds, respectively. Depending on the glass shard sizes, a 5, 10, 15, 20, or 25 µm-diameter beam was used. The analytical precisions determined from 12 replicate analyses of standard glass VG-568 were (in wt.%) SiO₂ ± 0.75, TiO₂ ± 0.02, Al₂O₃ ± 0.33, FeO ± 0.06, MnO ± 0.01, MgO ± 0.05, CaO ± 0.02, Na₂O ± 0.71, K₂O ± 0.07, F ± 0.10, Cl ± 0.02, P₂O₅ ± 0.02, and SO₂ ± 0.01.

The instability of Na during EMP analysis can result in a significant reduction in the intensity of its peak count rate (Keller 1981; Neilson and Sigurdsson 1981; Hunt and Hill 1993). Low probe currents, large beam diameter, and short counting time were used to minimize Na loss.

Analyses of volcanic glass shards often have low analytical totals, primarily because of water dissolved in the glass and Na loss. The water content of the glass cannot be determined by EMP. Typically, volcanic glasses have low (<0.5 wt.%) water contents at the time of eruption as water is insoluble in magmas at atmospheric pressures and is degassed during eruption. Volcanic glass is very reactive, and post-eruption hydration often increases water contents to many weight percent. Microprobe analyses were recalculated to correct for low analytical totals and to allow comparison between samples. Analyses were normalized to 100% after eliminating those with totals <90%. Because Na loss varies between glass shards in a single probe mount, the two to three highest Na₂O values from shards were averaged, excluding any obvious high outlier. The average Na₂O was used for each sample and then renormalized to 100% holding the Na₂O values constant for all analyses of glass shards from the sample. In the tables where multiple tephra samples were analysed, the standard deviation (SD) uncertainty (1 SD) is reported for all elements except Na₂O. In samples where Na₂O was not normalized, there is a listed SD for the analyses.

Neutron activation analyses (INAA)

Unprocessed dried bulk samples of 64 tephra were analysed by INAA to evaluate the possibility of using bulk tephra samples to characterize eruptions without the need for a lot of sample preparation. Approximately 100 mg samples were irradiated for 24–36 hours at a neutron flux of 2.4×10^{13} neutrons/second/cm² and then counted on high purity Ge detectors (Lindstrom and Korotev 1982; Hallett and Kyle 1993). NIST fly ash standard

1633a was used for calibration (Korotev 1987). The precision of the analyses varies from ~1 to 10% depending on the element in question. Standard reference rocks G-2 and BCR-1 were run to monitor the calibration during the analytical sessions.

Major element glass compositions

Data

We analysed 89 tephra samples from 27 known eruptions for their major and minor element compositions by EMP. The sample locations, ^{14}C ages (rounded to 50 years), distance and direction of the sample sites from their eruption vents, and average grain size are given in Table S1. Sample locations are also shown in Figures 1–5. In most cases, multiple samples were analysed from the same tephra to ensure uniformity in the tephra compositions and indirectly as a test of the field correlations. We attempted to analyse samples from proximal and distal locations where possible. When the tephra compositions were uniform and homogeneous, all the individual analyses were averaged, and a SD was calculated. In most cases, the SDs were <2 times the expected analytical uncertainty for most elements and were a test of the homogeneity of the samples.

Analyses reveal that 79 of the 89 ash samples have homogeneous glass compositions, with acceptably low SDs for most elements (Tables 1–5). For each of the homogeneous tephra, between 1 and 10 individual samples were analysed and averaged together to give a mean composition for the glass in the tephra. The number of individual microprobe analyses of glass shards ranged between 3 (SH_{2800}) and 79 (KS_1) for the individual eruptions.

Four of the 27 tephra samples have mixed compositions. In the case of the AV_1 and KS_2 tephra, this is evidenced by $\text{SD} > 1 \text{ wt.}\%$ for two or more elements within a single sample. No mean or SD were calculated for these tephra, and the individual analyses or means and SD of like samples are listed in the tables. Analyses reveal that the KHG and KSht_3 tephra have several distinct glass populations, and means and SDs are calculated for the individual populations.

Shiveluch volcano tephra (SH)

Twenty-three tephra samples representing 13 eruptions of Shiveluch volcano were analysed (Table 1). The tephra span eruption ages from calendar year 1964 to 5600 ^{14}C year BP (Table S1). All the glasses are rhyolitic in composition (Figure 6). The predominant bulk compositions of eruptive products from Shiveluch are hornblende phenocryst-rich high-Mg andesite (Ponomareva *et al.* 2007b). The groundmass glasses in the andesites are rhyolitic, and it was this low-density material that was dispersed during the eruptions. The dense minerals were deposited closer to the vent as crystal-rich tephra. It is important to note that, although the glasses are rhyolitic, the eruptions were andesitic. The rhyolitic composition of the glasses can be suggestive of larger eruptions; however, most Shiveluch eruptions are under a few cubic kilometres. The relatively small eruption size is consistent with the bulk andesitic compositions of Shiveluch eruptions.

Glass compositions for the Shiveluch tephra are similar (Table 1) and rhyolitic on the total alkali-silica (TAS) classification diagram (Figure 6). The SH_{2800} tephra glass has lower Na_2O and higher CaO compared to the other SH tephra layers, but as only three glass shards were analysed, these small differences are possibly analytical and may reflect the small

Table 1. Average microprobe analyses of glass from Shiveluch tephra layers.

Eruptive centre	SH ₁₉₆₄	SH ₁₈₅₄	SH ₁	SH ₂	SH ₃	SH ₄₅₀	SH ₆₀₀	SH ₅	SH ₂₈₀₀	SH ₃₅₀₀	SH _{dV}	SH ₄₇₀₀	SH ₅₆₀₀
Age (¹⁴ C BP)	-		250	950	1400	1450	1600	2550	2800	3500	4100	4700	5600
Number of samples analysed/N	1/6	1/11	3/21	4/25	3/33	2/13	1/6	3/16	1/3	1/7	1/9	1/11	1/4
SiO ₂	75.82	75.63	75.53	75.67	76.03	76.30	74.84	76.51	75.71	76.64	75.54	75.77	75.30
TiO ₂	0.22	0.08	0.25	0.23	0.24	0.26	0.31	0.23	0.32	0.22	0.30	0.25	0.26
Al ₂ O ₃	13.79	0.21	13.65	13.50	13.61	13.35	14.07	13.36	14.69	14.09	14.15	13.62	14.24
FeO	1.33	0.23	1.34	1.19	1.22	1.14	1.49	1.11	1.58	1.18	1.33	1.23	1.29
MnO	0.07	0.04	0.04	0.03	0.04	0.02	0.00	0.05	0.01	0.03	0.03	0.04	0.04
MgO	0.37	0.13	0.33	0.27	0.28	0.20	0.31	0.26	0.32	0.22	0.45	0.26	0.30
CaO	1.29	0.12	1.33	1.22	1.20	1.04	1.45	1.12	1.68	1.19	1.30	1.18	1.47
Na ₂ O ^a	3.97	4.36	4.39	4.67	4.33	4.45	4.42	4.24	2.47	3.47	3.83	4.72	4.33
K ₂ O	2.85	0.05	2.79	2.94	2.80	2.96	2.73	2.89	2.87	2.73	2.81	2.69	2.54
P ₂ O ₅	0.03	0.03	0.04	0.02	0.03	0.03	0.04	0.04	0.06	0.05	0.05	0.04	0.04
SO ₂	0.01	0.02	0.02	0.02	0.02	0.02	0.01	0.01	0.01	0.01	0.02	0.02	0.03
F	0.09	0.10	0.08	0.09	0.06	0.05	0.16	0.06	0.08	0.08	0.05	0.05	0.03
Cl	0.15	0.06	0.14	0.06	0.15	0.17	0.15	0.12	0.19	0.11	0.12	0.13	0.11
Total	100.00	100.00	100.00	100.00	100.00	100.00	100.00	100.00	100.00	100.00	100.00	100.00	100.00

Errors are 1σ. N=number of analyses averaged.
^aNa₂O values were normalized (see text).

Table 2. Average microprobe analyses of glass from homogeneous Kamchatka tephra.

Eruptive centre	KZ	KRM	IAv2	OP _{tr}	OP	KHD	KS ₁	KS ₃	IL	KO										
Age (¹⁴ C BP)	7550	7900	7150	4600	1500	2500	1800	6400	4850	7600										
Number of Samples analysed/N	4/25	3/38	2/12	3/37	5/55	5/39	10/79	2/12	1/8	8/59										
SiO ₂	77.07	0.30	74.69	0.28	75.08	0.35	76.37	0.27	76.94	0.34	74.90	0.31	73.74	0.54	70.37	0.42	66.12	1.01	76.39	0.73
TiO ₂	0.24	0.04	0.39	0.03	0.19	0.02	0.11	0.03	0.10	0.03	0.28	0.03	0.39	0.04	0.64	0.03	0.68	0.04	0.23	0.04
Al ₂ O ₃	12.75	0.25	13.47	0.16	14.54	0.17	13.68	0.17	13.15	0.27	13.98	0.25	14.23	0.28	14.61	0.22	15.82	0.43	13.15	0.43
FeO	1.31	0.06	1.86	0.10	1.60	0.07	0.75	0.04	0.62	0.06	1.60	0.06	2.56	0.18	4.35	0.17	4.85	0.40	1.52	0.09
MnO	0.03	0.03	0.04	0.03	0.08	0.04	0.05	0.04	0.09	0.04	0.07	0.04	0.11	0.04	0.16	0.05	0.15	0.02	0.06	0.04
MgO	0.24	0.09	0.36	0.09	0.43	0.02	0.13	0.06	0.06	0.03	0.37	0.09	0.46	0.07	0.87	0.05	1.88	0.26	0.27	0.09
CaO	1.59	0.06	1.49	0.08	2.78	0.10	0.92	0.06	0.67	0.07	1.65	0.08	2.11	0.15	3.05	0.11	4.96	0.31	1.52	0.13
Na ₂ O ^a	3.48		4.33		3.69		3.86	0.10	4.16		4.51		4.71		4.30		3.58	0.12	4.52	
K ₂ O	3.04	0.09	3.01	0.09	1.35	0.06	3.96	0.09	4.00	0.09	2.41	0.08	1.41	0.06	1.24	0.05	1.47	0.10	2.09	0.13
P ₂ O ₅	0.03	0.03	0.05	0.03	0.05	0.02	0.03	0.02	0.02	0.02	0.05	0.02	0.06	0.03	0.15	0.03	0.16	0.04	0.03	0.02
SO ₂	0.02	0.02	0.02	0.02	0.02	0.02	0.01	0.02	0.01	0.01	0.01	0.01	0.01	0.01	0.04	0.01	0.06	0.01	0.01	0.02
F	0.05	0.08	0.08	0.08	0.08	0.07	0.06	0.07	0.07	0.08	0.04	0.05	0.06	0.09	0.08	0.08	0.12	0.03	0.06	0.07
Cl	0.16	0.02	0.22	0.10	0.09	0.04	0.08	0.02	0.10	0.02	0.13	0.02	0.15	0.03	0.14	0.03	0.14	0.07	0.14	0.02
Total	100.00	100.00	100.00	100.00	100.00	100.00	100.00	100.00	100.00	100.00	100.00	100.00	100.00	100.00	100.00	100.00	100.00	100.00	100.00	100.00

Errors are 1σ. N-number of analyses averaged.

^a Where there is a standard deviation given, it means the Na₂O values were not normalized (see text).

Table 3. Microprobe analyses of glass from Khangar (KHG) tephra.

Sample	98032/2		KHG		98032/4		98121		98052/1		98106		99098/2	
N	7		7		7		7		8		13		7	
SiO ₂	76.41	0.40	76.63	0.44	77.15	0.37	76.76	0.36	77.30	0.41	77.49	0.39	77.28	0.36
TiO ₂	0.24	0.02	0.22	0.05	0.18	0.04	0.19	0.04	0.15	0.04	0.10	0.03	0.11	0.03
Al ₂ O ₃	13.38	0.21	13.30	0.26	13.08	0.22	13.22	0.21	13.08	0.18	12.81	0.23	13.09	0.16
FeO	1.10	0.15	1.11	0.09	0.96	0.06	1.01	0.13	0.79	0.15	0.63	0.06	0.62	0.04
MnO	0.04	0.04	0.06	0.04	0.02	0.02	0.04	0.05	0.04	0.03	0.05	0.04	0.05	0.04
MgO	0.27	0.03	0.28	0.05	0.23	0.04	0.23	0.05	0.15	0.05	0.07	0.02	0.08	0.04
CaO	1.29	0.12	1.28	0.11	1.18	0.11	1.10	0.07	0.95	0.12	0.78	0.04	0.75	0.05
Na ₂ O ^a	4.03		3.80		3.80		3.80		3.92		3.92		3.80	
K ₂ O	3.04	0.15	3.14	0.17	3.22	0.11	3.46	0.18	3.49	0.22	4.01	0.14	4.08	0.22
P ₂ O ₅	0.03	0.02	0.05	0.03	0.04	0.03	0.03	0.02	0.03	0.05	0.02	0.02	0.01	0.01
SO ₂	0.00	0.01	0.03	0.02	0.02	0.02	0.01	0.01	0.07	0.02	0.01	0.01	0.01	0.01
F	0.07	0.06	0.03	0.05	0.05	0.06	0.07	0.08	0.03	0.01	0.04	0.05	0.05	0.09
Cl	0.09	0.05	0.07	0.02	0.07	0.02	0.06	0.03	0.01	0.01	0.07	0.02	0.07	0.01
Total	100.00		100.00		100.00		100.00		100.00		100.00	100.00	100.00	

Errors are 1σ. N-number of analyses averaged.

^aNa₂O values were normalized (see text).

number of analyses. The main major element characteristics of the Shiveluch tephra are their medium K₂O contents (2.54 ± 0.14 to 2.96 ± 0.22 wt.%) (Figure 7).

KZ, KRM, OP_{tr}, OP, KHD, IL, KO tephra

Glass compositions in KZ, KRM, OP_{tr}, OP, KHD, IL, and KO tephra are homogeneous. On a total alkali-silica diagram (Figure 6), all the glasses are rhyolites except for IL, which is dacitic. The most diagnostic feature of the glasses is their K₂O contents. OP and OP_{tr} are classified as high K₂O (>3.5 wt.%); KHD, KZ, and KRM have medium K₂O (2.4–3.5 wt.%); and IL and KO have low K₂O (1.4–2.1 wt.%).

The bulk composition of the 4850 ¹⁴C year BP eruption from Iliinsky was andesitic, and on the basis of a single sample, the glass in the tephra is dacitic (Table 2, Figure 6). The dacitic composition and relatively low K₂O content (1.47 wt.%) are the most characteristic features of this tephra.

The KO eruption that formed the Kurile Lake caldera (Ponomareva *et al.* 2004) was the largest Holocene eruption in Kamchatka. We analysed eight tephra samples collected at distances of 50–1080 km from the caldera. The average of 59 glass analyses shows that the fall tephra are homogeneous and have a low K₂O rhyolite in composition.

Khangar (KHG)

Glasses from seven tephra samples erupted from Khangar all have rhyolitic compositions (Table 3, Figure 6). The glasses represent three distinct compositions and are here referred to as HK-KHG (high K₂O) with ~4 wt.% K₂O, MK1-KHG (medium K₂O#1) with ~3.5 wt.% K₂O, and MK2-KHG (medium K₂O#2) with ~3.15 wt.% K₂O. As there are no mixed populations of glass in the seven samples, we do not think the tephra resulted from a mixed magma eruption. The eruptive history of Khangar is not well known, and tephra

Table 4. Microprobe analyses of glass in samples of Avachinsky AV₁ tephra.

Sample	99163/10					99209/4					99209/5								
	N=5	N=5	N=5	N=5	N=5	7	6	2	8	4	5	3	2	9	7	10	8	1	6
SiO ₂	61.19	0.62	60.33	0.45	68.29	70.12	70.96	74.59	74.84	61.15	61.53	61.63	62.31	63.73	67.86	72.53	73.73	74.40	74.78
TiO ₂	0.80	0.05	0.93	0.04	0.95	0.39	0.48	0.43	0.39	0.87	0.92	0.93	0.95	0.74	0.50	0.41	0.39	0.47	0.40
Al ₂ O ₃	18.49	0.86	17.36	0.62	15.02	16.51	14.78	14.49	13.93	16.62	16.39	16.50	16.00	16.25	16.40	15.42	15.20	15.39	15.31
FeO	5.48	0.37	6.62	0.45	6.33	3.13	3.86	2.71	2.55	7.79	7.74	7.85	7.23	6.63	4.51	3.95	3.63	3.22	3.58
MnO	0.13	0.03	0.13	0.04	0.12	0.08	0.10	0.03	0.05	0.23	0.24	0.09	0.25	0.17	0.17	0.15	0.14	0.07	0.11
MgO	1.72	0.29	2.68	0.34	1.92	0.82	1.17	0.72	0.76	2.75	2.65	2.71	2.48	2.28	1.10	0.69	0.58	0.52	0.53
CaO	6.45	0.37	6.76	0.27	3.65	4.49	3.56	2.99	2.71	6.37	6.36	6.24	6.04	5.80	4.24	3.05	2.82	2.35	2.55
Na ₂ O	4.30	0.11	3.83	0.09	1.71	2.70	3.01	2.23	2.86	2.98	2.95	2.95	3.59	3.00	3.77	2.06	1.87	1.87	1.19
K ₂ O	1.03	0.05	1.02	0.03	1.56	1.44	1.74	1.65	1.71	0.78	0.75	0.70	0.82	0.80	1.07	1.33	1.32	1.36	1.32
P ₂ O ₅	0.18	0.04	0.15	0.06	0.19	0.04	0.20	0.05	0.07	0.25	0.19	0.27	0.16	0.29	0.12	0.10	0.07	0.07	0.08
SO ₂	0.01	0.01	0.03	0.02	0.00	0.02	0.02	0.00	0.00	0.05	0.06	0.02	0.05	0.08	0.02	0.03	0.02	0.01	0.00
F	0.11	0.07	0.06	0.07	0.12	0.13	0.00	0.00	0.03	0.03	0.03	0.00	0.00	0.12	0.13	0.10	0.07	0.13	0.00
Cl	0.10	0.02	0.11	0.02	0.14	0.13	0.12	0.12	0.10	0.12	0.19	0.11	0.12	0.11	0.13	0.17	0.17	0.14	0.14
Total	100.00	100.00	100.00	100.00	100.00	100.00	100.00	100.00	100.00	100.00	100.00	100.00	100.00	100.00	100.00	100.00	100.00	100.00	100.00

Errors are 1σ. Analysis number or N – number of analyses averaged;

Table 5. Electron microprobe analyses of glass in tephra from the 1907 Ksudach KSht₃ eruption.

Number of samples analysed/N	2/10		3/8	
SiO ₂	74.13	0.26	72.90	0.41
TiO ₂	0.29	0.03	0.33	0.05
Al ₂ O ₃	13.86	0.12	14.09	0.32
FeO	2.96	0.10	3.47	0.14
MnO	0.12	0.02	0.14	0.03
MgO	0.27	0.03	0.40	0.09
CaO	1.84	0.09	2.10	0.17
Na ₂ O ^a	4.72		4.82	
K ₂ O	1.43	0.04	1.42	0.03
P ₂ O ₅	0.05	0.03	0.05	0.04
SO ₂	0.02	0.04	0.02	0.01
F	0.13	0.16	0.08	0.06
Cl	0.18	0.02	0.17	0.03
Total	100.00		100.00	

Errors are 1σ. N-number of analyses averaged.
^a Na₂O values were normalized (see text).

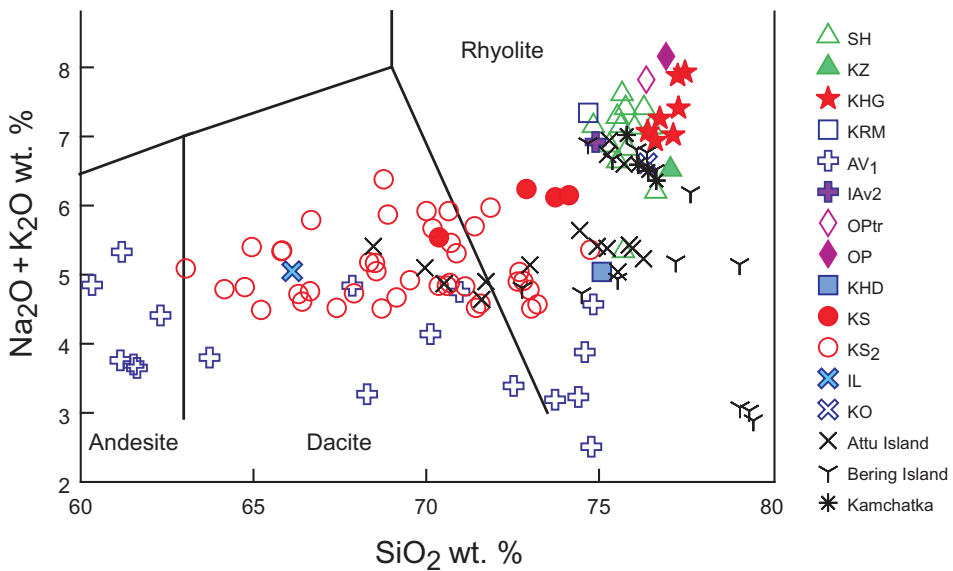


Figure 6. Total alkali (Na₂O + K₂O) versus silica (SiO₂) diagrams (Le Bas *et al.* 1986) of electron microprobe analyses of glass in tephra from known Kamchatka Holocene eruptions. All analyses are normalized to 100% on a volatile free basis; after Na normalized to account for volatilization during microprobe analyses.

correlations are tentative. We conclude that the glass compositions probably represent three distinct eruptions of Khangar that were closely spaced in time. Radiocarbon ages of 6600 and 6850 ¹⁴C year BP (Bazanova and Pevzner 2001) have been interpreted as representing at least two distinct eruptions.

Avachinsky (AV₁, IAv2)

We analysed glass from two tephra erupted from Avachinsky with volumes >1 km³. The oldest tephra IAv2 has homogeneous rhyolitic glass (Table 2). Glass shards from the younger AV₁ tephra are heterogeneous and range from andesite to rhyolite (Table 4; Figure 6). The most characteristic feature of the Avachinsky glasses is their low K₂O contents. IAv2 has a K₂O content of 1.35 wt.% (Table 2), and the heterogeneous AV₁ has glasses with K₂O contents ranging from 0.70 to 1.74 wt.% (Table 4).

Ksudach (KSht₃, KS₁, KS₂, KS₃)

Glasses in the KS₁ and KS₃ tephra are homogeneous. KS₁ glass is rhyolitic, whereas the glass in KS₃ tephra is dacitic (Table 2, Figure 6). Glass in KS₂ is heterogeneous and ranges from andesite to rhyolite in composition (Table S2, available with the online version of this article at <http://www.informaworld.com/tigr>, Figure 6). The pumice of the 1907 KSht₃ eruption is known to be heterogeneous and to vary from rhyodacite to andesite in composition (Volynets *et al.* 1999). We analysed glass from five tephra samples of KSht₃ (Table 5), and these fall into two distinct populations. Both populations are rhyolitic and have identical K₂O contents, but one is slightly more basic with lower SiO₂ and higher FeO and CaO (Figure 7).

Bulk INAAs of tephra

Sixty-four bulk tephra-fall samples (Table S3, available with the online version of this article at <http://www.informaworld.com/tigr>) erupted from 10 volcanic centres and representing 19 known Holocene eruptions were analysed (Table 6). We examined the trace element analyses of bulk samples to determine whether they could be used to derive a geochemical fingerprint. Fifteen tephra samples from unknown eruptions were also analysed to help with tephra identification. Sample 92319/3 from the KS₂ eruption was analysed in triplicate, and the mean and SD of the mean are listed in Table 6 and give a good indication of the analytical uncertainty.

As might be expected, some of the analyses of bulk tephra samples representing the various volcanic centres show a spread in their trace element compositions; however, data from some centres are tightly grouped together (Figure 8). Shiveluch tephra show the widest scatter in trace elements as represented by 11 samples. In contrast, the 14 samples representing the KS₁ and KS₂ eruptions are extremely tightly grouped. This is surprising because glasses from KS₂ tephra are extremely variable (Table S2) and range from dacite to rhyolite (Figure 6). Nineteen tephra samples (AV) erupted from Avachinsky volcano and representing five major eruptions show only a small spread in Th and La/Yb (Figure 8). This is surprising as the major element compositions of glasses from the AV₁ eruption are variable and also significantly different from the homogeneous IAv2 tephra (Figure 7). The four samples of KO tephra and the three samples of KRM tephra have diagnostic small variations in their La/Yb ratios but a great spread in their Th contents (Figure 8).

Tephra erupted from Shiveluch (SH) have a wide range in trace element contents (Table 6; Figure 8). This is in sharp contrast to the glass analyses (Table 1) that are uniform and cannot be used to distinguish any of the SH tephra from each other. Because the INAAs were made on bulk samples, the compositions will be affected by their crystal contents. Hornblende is an abundant phase in all the SH eruptive products and is common

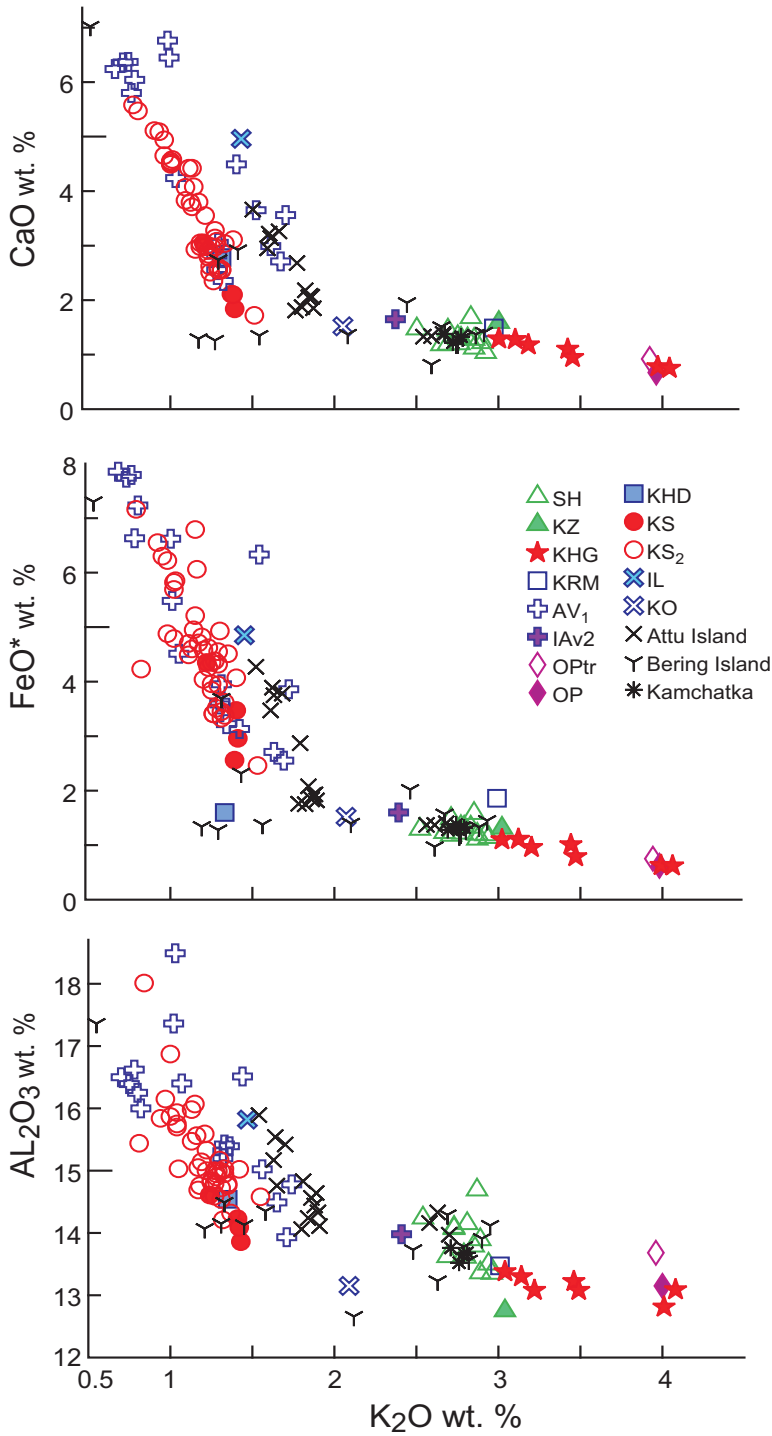


Figure 7. Major element variation diagrams of electron microprobe analyses of glass in tephra from Holocene eruptions in Kamchatka. All analyses are normalized to 100% on a volatile free basis; after Na normalized to account for volatilization during microprobe analyses.

Table 6. Neutron activation analyses of bulk tephra samples.

Sample	345/I	345/II	80004/3	345/4	345/5	90116/8	80006/5	80013/12	90077/1	345/7	1040/1	8300	SH ₈₃₀₀	K-1/7	K-1/8	K-1/9	80013/4	345/9	85220/1	
Eruption	SH ₂	SH ₂	SH ₂	SH ₃	SH ₁₄₅₀	SH ₅	SH ₈₃₀₀	KZ	KZ	KZ	KZ	KZ	KZ	KZ	KZ	KHG				
¹⁴ C year BP	950	950	950	1400	1400	1400	1400	1400	1450	2550	8300	7550	7550	7550	7550	7550	7550	7550	7550	6850
DNa ₂ O	4.25	4.44	4.48	4.27	4.52	4.55	4.43	4.12	3.97	4.25	3.58	3.44	3.17	3.47	3.20	3.25	3.25	3.25	3.25	4.28
Sc	10.83	20.77	9.96	11.26	17.50	18.78	6.35	10.39	16.23	18.06	13.71	12.44	11.13	18.80	8.97	13.00	13.00	13.00	13.00	6.46
Cr	90	161	87	132	160	166	47	98	152	173	67	14	10	18	13	30	30	30	30	17
IFeO	4.25	6.03	3.95	4.27	5.22	5.59	2.53	3.93	5.76	5.80	4.91	5.50	4.20	7.02	3.29	4.06	4.06	4.06	4.06	2.85
Co	13.5	23.7	13.0	14.0	20.3	21.6	8.1	12.7	19.5	21.2	14.2	13.2	10.4	18.4	7.6	12.3	12.3	12.3	12.3	6.3
Zn	60	85	52	64	65	65	37	58	70	78	49	54	47	64	38	50	50	50	50	49
As	10.3	1.3	11.2	9.9	2.2	2.6	13.7	9.1	7.1	4.4	8.1	2.7	2.9	1.1	3.6	2.9	2.9	2.9	2.9	1.7
Br	1.9	0.2	2.8	3.4	0.7	1.4	7.4	4.4	30.5	1.5	7.3	3.3	5.1	1.7	7.3	5.4	5.4	5.4	5.4	1.5
Rb	35	9	39	32	7	7	42	32	19	15	26	31	37	16	46	39	39	39	39	43
Sb	0.9	0.2	1.0	0.9	0.3	0.2	1.1	0.8	0.5	0.4	0.6	0.3	0.2	0.1	0.3	0.3	0.3	0.3	0.3	0.1
Cs	1.41	0.40	1.65	1.33	0.28	0.30	1.78	1.37	0.87	0.56	1.25	1.27	1.53	0.66	2.05	1.62	1.62	1.62	1.62	1.18
Ba	514	220	568	495	252	279	590	499	335	318	424	533	642	382	782	687	687	687	687	636
La	10.03	6.28	8.71	8.89	5.65	5.67	9.82	7.55	6.80	6.12	8.74	10.10	11.60	8.30	12.69	10.84	10.84	10.84	10.84	21.46
Ce	21.7	16.3	19.2	18.7	13.6	13.8	21.7	16.9	16.5	15.5	19.5	21.0	24.1	19.1	27.3	22.9	22.9	22.9	22.9	44.0
Nd	10.3	11.3	9.6	9.2	8.3	9.1	9.1	7.3	9.9	8.0	10.1	9.5	9.1	11.4	14.6	10.5	10.5	10.5	10.5	19.1
Sm	2.62	3.25	2.29	2.38	2.71	2.82	1.90	2.10	2.62	2.56	2.79	2.65	2.74	3.25	2.80	2.76	2.76	2.76	2.76	3.88
Eu	0.70	1.08	0.62	0.69	0.92	0.93	0.53	0.62	0.85	0.88	0.81	0.86	0.83	1.09	0.78	0.82	0.82	0.82	0.82	0.92
Tb	0.33	0.50	0.30	0.30	0.37	0.41	0.28	0.31	0.38	0.40	0.44	0.41	0.44	0.55	0.43	0.43	0.43	0.43	0.43	0.49
Yb	1.19	1.57	1.19	1.16	1.26	1.33	0.99	1.07	1.42	1.35	1.46	1.71	1.72	2.02	1.84	1.85	1.85	1.85	1.85	1.79
Lu	0.19	0.23	0.21	0.18	0.19	0.20	0.15	0.17	0.19	0.19	0.22	0.27	0.28	0.31	0.29	0.28	0.28	0.28	0.28	0.31
Hf	3.73	2.26	3.95	3.48	1.76	1.93	4.20	3.59	3.04	2.43	3.99	3.37	3.22	2.68	4.09	3.37	3.37	3.37	3.37	4.10
Ta	0.17	0.10	0.23	0.17	0.09	0.23	0.09	0.18	0.16	0.10	0.22	0.29	0.31	0.22	0.40	0.36	0.36	0.36	0.36	0.74
Th	1.63	0.39	1.99	1.43	0.37	0.36	2.03	1.45	1.04	0.66	1.75	2.18	2.75	1.14	3.49	2.57	2.57	2.57	2.57	4.11
U	0.9	0.3	0.9	0.8	0.2	0.1	1.2	0.8	0.6	0.4	1.1	1.2	1.5	0.7	2.0	1.4	1.4	1.4	1.4	2.3

Sample	1039/3	87209/2	345/8	92319/C	8403/5	5ab/4	1176/87	89168/8	8408/7	80625/1	80012/5	91149/13	86684/4	89161/7	89167/6
Eruption	KHG	KHG	KHG	KRM	KRM	KRM	AV ₁	AV ₂	AV ₂	AV ₃	AV ₃				
¹⁴ C year BP	6850	6850	6850	7900	7900	7900	3500	3500	3500	3500	3500	4000	4000	4500	4500
INa ₂ O	3.57	3.78	3.68	4.18	3.69	6.35	3.09	2.62	2.98	3.02	3.12	3.52	3.27	3.61	2.60
Sc	9.54	9.43	8.28	9.98	15.36	15.67	31.60	41.10	28.56	24.00	24.45	16.02	23.23	13.41	28.55
Cr	19	13	21	7	8	9	8	38	17	10	17	13	19	4	35
IFeO	3.69	3.51	3.00	3.08	4.62	4.80	9.16	9.86	8.74	7.02	6.89	6.49	5.15	5.99	9.09
Co	8.6	8.8	6.8	6.0	12.7	8.7	24.8	29.2	23.1	17.8	18.7	15.1	16.2	12.2	21.7
Zn	75	53	59	101	63	73	86	95	83	66	74	90	83	74	105
As	3.8	4.8	4.6	3.2	5.5	5.1	3.2	4.2	4.7	5.3	5.5	4.4	2.7	5.9	4.2
Br	9.1	12.2	2.5	4.4	2.0	5.6	0.7	4.6	4.9	5.2	4.4	0.6	1.6	1.0	8.1
Rb	37	43	48	32	32	49	6	5	7	7	7	11	7	10	9
Sb	0.2	0.3	0.3	0.3	0.5	0.5	0.3	0.2	0.7	0.3	0.4	0.3	0.2	0.4	0.2
Cs	1.33	1.84	1.51	1.30	1.42	1.95	0.60	0.48	0.58	0.62	0.67	0.80	0.45	0.76	0.30
Ba	550	505	831	492	450	719	214	162	201	188	264	282	233	290	129
La	17.35	16.14	18.76	12.05	11.97	17.36	4.11	3.31	3.63	4.88	5.07	5.51	4.11	5.87	3.34
Ce	37.4	34.0	40.1	29.6	27.6	40.6	9.9	8.5	9.7	12.8	11.9	13.6	10.7	14.4	8.1
Nd	17.6	13.2	17.4	18.0	16.0	20.1	7.3	6.4	6.5	7.6	8.1	8.3	7.0	9.0	5.7
Sm	3.79	3.12	3.71	3.94	3.96	5.64	2.54	2.36	2.22	2.76	2.76	2.57	2.33	2.86	2.16
Eu	0.99	0.92	0.88	0.94	1.07	1.42	0.86	0.80	0.82	0.94	0.92	0.86	0.84	0.87	0.79
Tb	0.55	0.47	0.50	0.65	0.66	0.92	0.53	0.54	0.47	0.58	0.57	0.48	0.45	0.51	0.45
Yb	1.97	2.14	1.92	2.68	2.65	4.22	1.98	1.88	1.83	2.31	2.02	1.97	1.78	2.09	1.85
Lu	0.30	0.35	0.29	0.43	0.39	0.63	0.29	0.29	0.26	0.35	0.31	0.29	0.28	0.33	0.25
Hf	3.75	4.56	4.46	5.25	4.80	7.83	1.78	1.59	1.85	2.29	2.22	2.41	1.76	2.70	1.25
Ta	0.74	0.79	0.80	0.30	0.24	0.40	0.00	0.05	0.07	0.08	0.11	0.00	0.09	0.10	0.00
Th	3.43	3.67	3.87	2.34	2.01	3.56	0.35	0.32	0.37	0.67	0.65	0.66	0.47	0.65	0.30
U	1.7	1.6	1.6	1.4	1.1	2.2	0.34	0.43	0.20	0.37	0.37	0.42	0.44	0.31	0.26
la/yb							20758	1.7606	1.9836	2.1126	2.5099	2.79695	2.309	2.80861	1.80541

(Continued)

Table 6. (Continued).

Sample	87242/3	89163/17	89168/4	8403/17	87242/7	87242/4	89163/16	89168/3	91168/3	1048/11	8408/8	8825/6	86042/6	86038/7	8880/5	1203/3
Eruption	AV ₃	AV ₄	AV ₅	AV ₅	AV ₅	AV ₅	OP	KHD	KHD	KS ₁	KS ₁	KS ₁				
¹⁴ C year BP	4500	5500	5500	5500	5500	5500	5600	5600	5600	5600	1500	2500	2500	1800	1800	1800
INa ₂ O	2.19	3.65	3.14	5.90	1.56	2.38	3.59	3.15	3.40	3.16	4.66	4.85	4.19	5.00	4.90	4.36
Sc	16.18	14.43	16.93	19.46	23.82	23.82	14.11	16.21	20.06	19.37	17.67	6.72	7.52	15.41	14.10	20.06
Cr	16	7	35	24	29	26	4	31	31	67	7	6	4	5	2	7
IFeO	5.52	5.77	6.38	8.48	4.05	3.57	5.78	6.36	5.75	4.59	4.77	2.36	1.92	3.31	2.96	4.88
Co	9.9	13.0	15.8	18.2	13.0	12.4	13.1	15.5	15.3	14.9	8.7	1.8	2.3	3.8	2.9	6.5
Zn	38	77	66	90	81	55	69	76	68	67	69	50	46	85	77	91
As	213.3	6.3	5.6	7.9	15.3	17.1	5.3	5.5	3.1	2.1	3.1	9.7	10.8	10.6	10.5	9.7
Br	1.6	1.1	12.0	11.9	0.9	0.3	0.8	10.6	4.9	0.8	4.1	4.1	2.8	1.9	5.7	7.4
Rb	20	15	16	10	11	3	15	11	7	5	25	41	41	21	22	18
Sb	1.2	0.4	0.4	0.4	0.5	0.3	0.5	0.4	0.3	0.2	0.2	0.5	0.5	0.6	0.5	0.4
Cs	1.81	0.93	0.70	0.60	0.70	0.37	0.88	0.74	0.59	0.34	1.05	1.86	2.11	1.66	1.71	1.38
Ba	388	389	343	257	289	187	386	311	258	234	441	517	487	338	359	298
La	7.37	7.17	6.31	5.22	4.54	3.28	7.01	6.43	4.99	4.33	10.89	12.11	11.15	8.41	8.91	6.85
Ce	17.6	16.5	13.7	11.5	10.1	8.6	15.3	15.3	14.0	9.5	25.5	28.5	26.8	21.9	24.0	19.0
Nd	8.4	9.3	7.6	7.6	5.8	6.0	9.6	8.5	6.0	5.5	14.4	14.3	17.7	15.8	19.4	13.3
Sm	2.59	2.89	2.69	2.48	1.94	2.28	2.72	2.63	2.40	1.71	3.99	4.34	4.22	5.33	5.76	4.69
Eu	0.81	0.88	0.84	0.83	0.51	0.76	0.84	0.84	0.86	0.73	1.21	1.03	0.97	1.30	1.27	1.34
Tb	0.41	0.51	0.53	0.55	0.38	0.47	0.48	0.48	0.40	0.32	0.70	0.77	0.71	1.11	1.17	0.96
Yb	1.61	2.17	2.00	2.07	1.59	1.95	1.93	1.84	1.79	1.37	2.88	3.50	3.42	4.94	5.10	4.07
Lu	0.24	0.32	0.29	0.30	0.26	0.31	0.31	0.29	0.26	0.22	0.44	0.57	0.54	0.75	0.78	0.61
Hf	2.58	2.81	2.66	2.32	2.07	2.16	2.68	2.52	1.89	1.36	4.38	5.06	4.78	4.61	4.88	3.86
Ta	0.22	0.12	0.10	0.09	0.11	0.09	0.11	0.12	0.08	0.06	0.22	0.21	0.22	0.13	0.13	0.11
Th	1.14	0.88	0.90	0.64	0.68	0.43	0.74	0.79	0.52	0.42	1.85	2.42	2.49	1.09	1.13	0.94
U	0.58	0.48	0.38	0.31	0.32	0.20	0.40	0.42	0.48	0.19	1.3	0.9	1.2	0.3	0.6	0.3
la/yb	4.5776	3.30415	3.155	2.52174	2.8553	1.6821	3.63212	3.4946	2.78771	3.16058						

Sample	1203/4	92285/4	80003/11	345/6	8811/1	86684/8	91160a/1	94431/1	92319/3	1053/1	87242/10	8645/1	1351/1	8841/7	86031/11	Mag-1
Eruption	KS ₁	KS ₁	KS ₁	KS ₁	KS ₂	IL	KO	KO	KO	KO						
¹⁴ C year BP	1800	1800	1800	1800	6000	6000	6000	6000	6000	n = 3	6000	4850	7600	7600	7600	7600
INa ₂ O	4.40	4.62	4.52	4.61	4.04	3.34	3.89	3.76	0.04	4.31	2.56	5.35	4.70	3.94	3.70	4.57
Sc	18.94	19.83	16.94	16.35	24.73	28.84	26.08	27.40	0.13	26.53	22.93	24.71	8.56	17.60	16.39	8.28
Cr	5	8	9	9	12	15	10	9	0.5	13	8	15	6	15	17	5
IFeO	4.38	5.14	3.94	3.79	5.06	7.59	6.80	7.13	0.02	5.29	3.31	6.37	1.94	4.36	4.39	1.54
Co	5.4	6.9	5.8	6.1	11.7	15.3	14.9	12.1	0.1	10.7	5.3	13.3	2.2	10.4	9.1	1.2
Zn	78	97	85	99	95	94	93	94	7	79	65	86	45	54	68	35
As	10.6	7.7	12.1	10.9	7.7	19.3	5.1	6.0	0.9	4.8	10.3	10.2	9.9	7.7	7.6	10.5
Br	9.2	4.5	3.3	3.7	2.9	13.1	27.6	8.7	0.2	1.5	1.4	4.4	2.2	12.3	25.7	2.3
Rb	16	17	22.5	21	13	5	12	10	1	12	14	31	33	17	24	37
Sb	0.4	0.4	0.5	0.5	0.9	0.3	0.3	0.3	0.0	0.3	0.5	0.4	0.5	0.5	0.3	0.3
Cs	1.40	1.43	1.84	1.58	1.28	1.05	1.03	0.96	0.02	0.98	1.94	1.75	2.1	1.22	1.48	2.29
Ba	329	321	405	393	270	256	294	206	6	253	169	417	449	263	373	455
La	7.60	6.67	7.55	7.83	7.15	5.44	5.83	5.62	0.16	5.47	4.31	11.35	10.45	6.69	7.77	10.94
Ce	21.0	17.2	21.4	20.6	21.2	14.7	15.9	15.6	0.1	15.9	12.1	28.4	25.4	15.5	19.1	26.9
Nd	14.0	15.6	15.6	13.7	10.2	13.1	14.1	12.4		12.4		14.7	14.4	9.3	10.8	14.7
Sm	4.89	4.03	4.94	5.00	3.89	4.08	4.04	3.68	0.03	3.88	2.87	4.56	3.92	2.86	2.63	4.13
Eu	1.36	1.27	1.55	1.28	1.29	1.38	1.37	1.32	0.01	1.36	1.09	1.35	0.94	1.18	0.97	0.90
Tb	1.01	0.82	1.02	1.05	0.97	0.80	0.82	0.78	0.02	0.83	0.60	0.87	0.71	0.54	0.50	0.77
Yb	4.19	3.86	4.49	4.58	4.40	3.22	3.38	3.17	0.05	3.32	2.52	3.62	3.75	2.60	2.27	3.92
Lu	0.64	0.60	0.69	0.66	0.69	0.50	0.52	0.48	0.01	0.51	0.41	0.58	0.58	0.42	0.35	0.59
Hf	3.97	3.90	4.40	4.30	4.14	3.01	3.32	3.22	0.07	2.75	3.51	5.16	5.27	3.27	3.57	5.24
Ta	0.14	0.14	0.15	0.13	0.11	0.10	0.13	0.10	0.01	0.10	0.17	0.20	0.22	0.15	0.14	0.21
Th	0.97	0.91	0.97	0.97	0.96	0.82	0.82	0.70	0.07	0.67	0.60	2.42	2.30	1.36	1.82	2.43
U	0.5	0.5	0.4	0.5	0.3	0.4	0.3	0.50	0.13	0.3	0.3	1.4	1.0	0.6	0.7	0.9

Elemental abundances in ppm and oxides in wt. %.

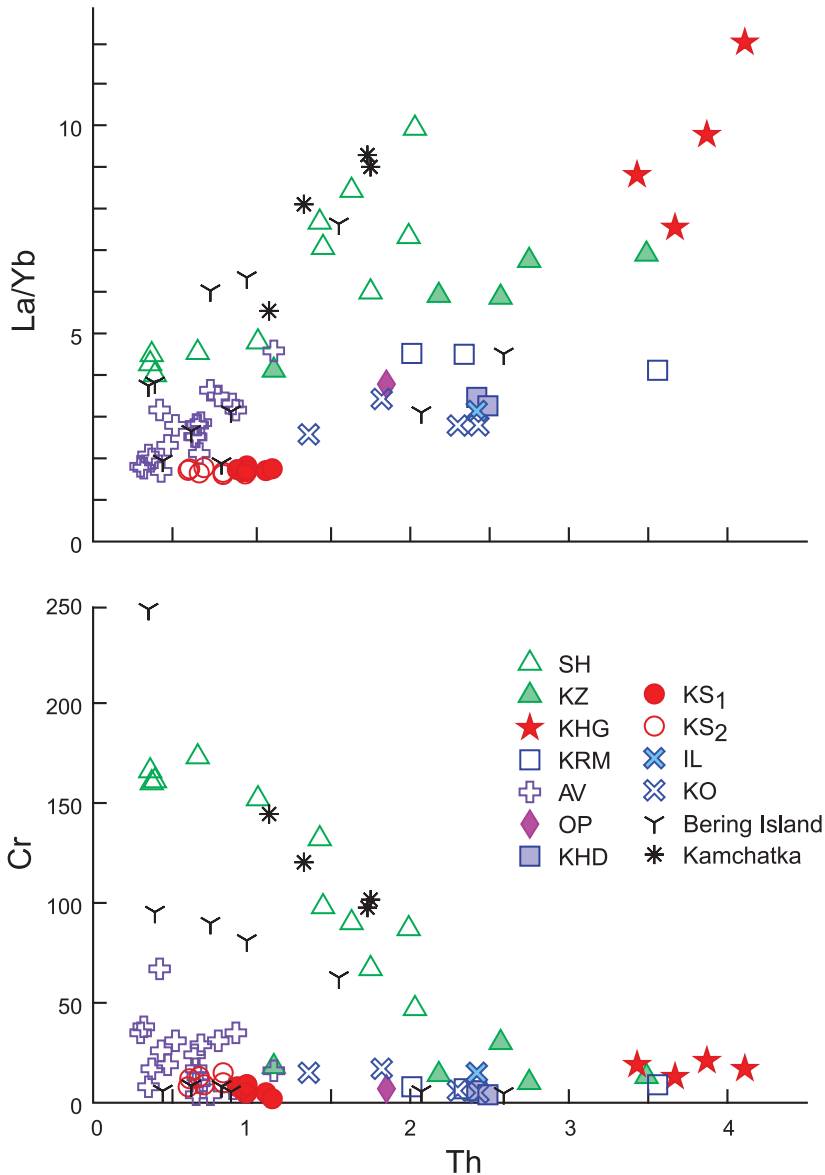


Figure 8. Trace element variation diagrams of bulk tephra samples.

in the tephra (Ponomareva *et al.* 2007b). The hornblende will be fractionated from the glass because of its greater density and settle out from the eruption plume closer to source. The four samples with the highest Cr contents are <50 km from the vent and are coarse ash, whereas four of the five samples with the lowest Cr content are fine ash and over 100 km from the source (Figure 8). Even the most distal glass-rich SH tephra have characteristically higher Cr contents than any other Kamchatka tephra. Four tephra from the Bering Island (Figure 8) have distinctly higher Cr contents than the other tephra on the island and are correlated with Shiveuch eruptions. It is noticeable that these four tephra do

have lower Cr contents at the equivalent Th content than those of the sample collected closer to the volcano. This is probably also owing to their long distance from the Shivelich volcano and fractionation of Cr-bearing mineral phases during transport.

Geochemical signatures of Kamchatka tephra

In the field, the known tephra layers analysed by EMP and INAA have been distinguished from one another on the basis of many parameters including stratigraphic position, proximity to a volcanic centre, physical properties, and ^{14}C ages. To date, no chemical or mineralogical fingerprint has been found to uniquely identify each tephra. This study is the first time that a systematic attempt has been made to use EMP analyses of glass supplemented by trace element analyses of bulk samples to characterize individual tephra layers. Glass is the most widespread component in the tephra, and their chemical compositions are the most diagnostic features that allow unique identification of eruptive centres and in some cases individual tephra layers.

K_2O shows the greatest variation amongst the glasses and is the primary chemical component used for identification. On the basis of the K_2O contents, we divide the tephra into three types: low (<2.5 wt.% K_2O), medium (>2.5 to <3.5 wt.%), and high (>3.5 wt.%) K_2O contents (Table 7; Figure 7). Where glasses have similar K_2O contents, other major elements especially CaO, FeO, and Al_2O_3 allow individual tephra to be identified (Table 7). The differences in the compositions of the glasses are such that statistical analyses of the data are not needed to identify a tephra, and the criteria given in Table 7 can be easily used. For example, using K_2O as the principal chemical fingerprint, the KZ and KRM

Table 7. Geochemical characteristics of Holocene tephra from Kamchatka.

Tephra	K_2O wt. %	CaO wt. %	FeO wt. %	Al_2O_3 wt. %	Cr (ppm)	La/Yb	Th (ppm)
High K_2O (>3.5 wt. %)							
OP	4.0	0.70	0.75	13.2	<50	~4	1.85
Op _{tr}	4.0	0.90	0.62	13.7			
HK-KHG	4.0	0.80	0.63	12.9	<50	>7	3.4–4.1
Medium K_2O (<2.5 to 3.5 wt. %)							
MK1-KHG	3.5	1.00	0.9	13.2	<50	>7	3.4–4.1
MK2-KHG	3.1	1.25	1.1	13.2	<50	>7	3.4–4.1
KZ	3.0	1.59	1.3	12.8	<50	6–7	2.0–3.5
KRM	3.0	1.49	1.9	13.5	<50	4–5	4.0–5.0
SH	2.5–3.0	1.0–1.5	1.1–1.5	13.3–14.2	>50	4–10	<2.05
Low K_2O (<2.5 wt. %)							
KHD	2.4	1.65	1.6	14.0	<50	3.0–3.5	2.4–2.5
KO	2.1	1.50	1.5	13.2	<50	2.5–3.5	1.4–2.4
IL	1.5	4.96	4.85	15.8	<50	3	2.4
IAv2	1.4	2.78	1.6	14.5			
KSht ₃	1.4	1.8–2.1	3.0–3.5	13.9–14.1			
KS ₁	1.4	2.10	2.60	14.2	<50	1.7–1.8	0.9–1.1
KS ₃	1.2	3.00	4.35	14.6			
KS ₂	0.8–1.4	2.6–5.6	3.4–7.2	14.2–16.9	<50	1.6–1.8	0.6–1.0
AV ₁	0.7–1.7	2.4–6.8	3.1–7.8	2.5–5.6	<50	1.7–2.5	0.3–0.7

Highlighted values are the most diagnostic for identifying an eruptive centre or eruption.

tephras are similar with 3.0 wt.% K₂O. The glasses are, however, easily identified using their distinct CaO and FeO contents (Table 7).

Trace element analyses of bulk samples have proved very useful in characterizing most of the 10 eruptive centres examined. Bulk samples of tephra erupted from Shiveluch volcano are all enriched with Cr compared to other Kamchatka eruptions (Figure 8). The tephra from Khangar (KHG) has a characteristic high Ta content. Hf/Ta ratios are also diagnostic of KHG and KZ tephra. We have selected plots of Cr and La/Yb versus Th (Figure 8) to illustrate the trace element signatures. The geochemical behaviour of Th is similar to K₂O, and hence it acts as a good proxy for K₂O. The trace element criteria we have used to aid in distinguishing the various tephra are summarized in Table 7.

Tephra of unknown origins

Samples

Nineteen tephra samples from Bering Island (10 tephra samples), Attu Island (five samples) in the Aleutians, Karaginsky Island (three samples), and Uka Bay (one sample) on mainland Kamchatka (Figure 1) were from unknown eruptions. We used their glass compositions to identify their eruptive sources. Bulk samples of the tephra from Karaginsky and Bering Islands and Uka Bay were also analysed for trace elements by INAA to supplement and complement the glass analyses. Details on the samples are given in Table 8 and analyses are listed in Tables 9 and 10.

Nine of the 10 Bering Island samples (numbered 93K63/-) were collected from the northern end of the island (Table 8). The tephra horizons were clearly recorded in a section through a Holocene peat bog and exhibited no evidence of redeposition (Kirianov *et al.* 1990). The stratigraphy of the section is shown in Figure 9. Tephra sample 93K60/1 was collected from the top of a coastal section, and it correlates with sample 93K63/1 (Table 8).

The Bering Island tephra cannot be correlated back to their volcanic source on the basis of their stratigraphy, but the stratigraphic sequence does provide a time series. ¹⁴C ages on bulk peat samples near the tephra do help with correlations (Kirianov *et al.* 1990).

Analytical data

Glass compositions in 17 of the 19 tephra samples from unknown sources are homogeneous and two have mixed compositions (Tables 9 and 10). All the samples are rhyolitic, except for 93K63/2 from Bering Island which has an andesitic glass composition. The tephra with mixed compositions come from Bering Island and Attu Island.

Identification

The unknown tephra samples from Bering, Attu and Karaginsky Islands, and Uka Bay are compared to known samples in the major and trace element plots (Figures 7 and 8).

Tephra layers 93K60/1 and 93K63/1

These tephra have an age of 1400–1500 ¹⁴C year BP based on dated peat beneath the 93K63/1 tephra (Kirianov *et al.* 1990). The K₂O, CaO, and FeO contents of the glasses (Figure 7) and high Cr contents (>50 ppm) of the bulk samples (Figure 8) are typical of

Table 8. Fine-ash tephra samples from unknown sources.

Section	Layer code	Sample code	Age estimate, ^{14}C years BP	Tentative correlation	Suggested correlation
Bering Island	KD-1	93-K63/1	1400–1500	Shiveluch	SH ₁₄₅₀
	KD-1	93-K60/1	1450–1500	Shiveluch	SH ₁₄₅₀
	–	93-K63/2	Somewhat younger than 3150 ± 170	not sampled	Avachinsky
	KD-2	93-K63/3		Shiveluch	SH ₂₈₀₀
	KD-3	93-K63/4	Between 3150 ± 170 and 3660 ± 100	Shiveluch	Shiveluch
	KD-4	93-K63/5		Shiveluch	Ksudach or Avachinsky
	KD-5	93-K63/6	Between 3880 ± 140 and 4790 ± 210	Shiveluch	SH _{dv}
	–	93-K63/7	$\sim 4790 \pm 210$	not sampled	Ksudach or Avachinsky
	KD-6	93-K63/8	$\sim 7110 \pm 90$	Shiveluch	IAV ₂
	KD-7	93-K63/9	Between 7440 ± 50 and 7610 ± 140	Kizimen	KO
Karaginsky Island	KD-8	93-K63/10	$\sim 7820 \pm 50$	KRM	KRM
		93-K38/1	Late Holocene	Shiveluch	SH ₁₈₅₄
		93-K30/1	Late Holocene	Shiveluch	Shiveluch
Northern Kamchatka, Uka Bay		93-K30/2	Late Holocene	Shiveluch	Shiveluch
		93-K50/1	$<160 \pm 40$	Shiveluch	SH ₁₈₅₄
Attu Island		95-02/1			
		95-01/1			
		95-01/3			
		95-01/2			
		95-06/1			

Note: Layer codes and tentative correlation for tephras on Bering Island according to Kirianov *et al.* (1990).

SH tephra. On the basis of age, the possible correlatives are SH₃ (1400 ^{14}C year BP) and SH₁₄₅₀ (1450 ^{14}C year BP). The tephra are correlated with the SH₁₄₅₀ eruption because the dispersal axis for the eruption (Figure 2E) was towards Bering Island, whereas the SH₃ eruption was directed S (Figure 2B).

Tephra layer 93K63/2

This tephra is <3150 ^{14}C year BP based on a dated peat underlying an older tephra (Figure 9, Table 8) (Kirianov *et al.* 1990). The glass is andesitic (Table 6) and homogeneous. The only andesitic glasses we have analysed were from the AV₁ eruption, but the AV₁ tephra is heterogeneous, which makes it difficult to be a correlative. However, the andesitic composition is typical of AV eruptions; hence the question remains which eruption? The INAA of the bulk sample has low Cr, Th, and La/Yb contents and plots in the AV field on the Th versus La/Yb variation diagram (Figure 8). The age is younger than that of AV₁ eruption (3500 ^{14}C year BP). As all the products of the Young Cone of Avachinsky volcano are basaltic andesite and similar to the initial AV₁ tephra (Bazanov *et al.* 2003), we suggest that 93K63/2 is most likely a product of an unknown Avachinsky eruption

Table 9. Microprobe analyses of glass and INAs of bulk samples of unidentified tephra from Kamchatka.

Sample	Karaginsky Island			Ulka Bay			Bering Island		
	93K30/1	93K30/2	93K38/1	93K50/1	93K60/1	93K63/1	93K63/2	93K63/3	93K63/4
N	8	8	13	9	6	15	4	6	6
SiO ₂	76.43 0.28	76.66 0.28	75.80 0.23	76.14 0.41	76.10 0.26	76.39 0.58	59.63 0.90	75.39 0.61	74.61 0.24
TiO ₂	0.25 0.03	0.26 0.04	0.24 0.04	0.26 0.04	0.24 0.02	0.21 0.03	0.97 0.07	0.32 0.03	0.30 0.02
Al ₂ O ₃	13.67 0.14	13.52 0.23	13.67 0.15	13.76 0.23	13.56 0.18	13.62 0.32	17.36 0.45	14.12 0.37	14.27 0.14
FeO	1.32 0.07	1.38 0.05	1.32 0.07	1.28 0.09	1.28 0.05	1.17 0.11	7.30 0.31	1.45 0.09	1.56 0.11
MnO	0.03 0.04	0.03 0.03	0.03 0.03	0.04 0.02	0.03 0.03	0.03 0.03	0.15 0.04	0.02 0.03	0.04 0.06
MgO	0.29 0.02	0.31 0.02	0.32 0.03	0.36 0.14	0.31 0.03	0.38 0.35	2.62 0.27	0.35 0.08	0.37 0.05
CaO	1.27 0.05	1.22 0.08	1.33 0.07	1.38 0.15	1.32 0.08	1.19 0.16	7.02 0.33	1.41 0.13	1.51 0.04
Na ₂ O ^a	3.71	3.60	4.21	3.88	3.99	3.99	4.02	3.72	4.30
K ₂ O	2.79 0.07	2.76 0.11	2.81 0.09	2.71 0.07	2.82 0.09	2.78 0.20	0.55 0.03	2.95 0.02	2.69 0.12
P ₂ O ₅	0.03 0.03	0.04 0.02	0.05 0.04	0.03 0.02	0.06 0.02	0.04 0.02	0.18 0.02	0.06 0.04	0.12 0.11
SO ₂	0.02 0.02	0.03 0.02	0.03 0.02	0.02 0.01	0.04 0.02	0.02 0.02	0.02 0.02	0.03 0.01	0.15 0.08
F	0.07 0.09	0.04 0.05	0.07 0.08	0.03 0.06	0.02 0.04	0.05 0.06	0.05 0.07	0.04 0.07	0.07 0.04
Cl	0.12 0.03	0.16 0.03	0.12 0.02	0.10 0.03	0.22 0.09	0.13 0.03	0.13 0.06	0.15 0.10	0.02 0.01
Total	100.00	100.00	100.00	100.00	100.00	100.00	100.00	100.00	100.00

Downloaded By: [Kyle, Philip] At: 04:20 5 May 2011

Location	Karaginsky Island			Ulka Bay			Bering Island		
	93K30/1	93K30/2	93K38/1	93K50/1	93K60/1	93K63/1	93K63/2	93K63/3	93K63/4
Sample	8	8	13	9	6	15	4	6	
Bulk analyses									
INa ₂ O	4.23	4.17	4.13	4.24	4.25	4.06	2.81	3.77	4.24
Sc	10.62	16.49	3.10	12.32	9.77	11.88	20.43	21.39	18.29
Cr	101.6	144.5	97.6	120.3	62.7	81.2	5.9	247	95.4
IFeO	4.06	5.46	3.10	5.50	2.59	2.80	5.23	4.41	3.86
Co	12.73	18.89	9.48	17.12	9.52	12.29	14.72	22.68	19.07
Zn	66	70	49	72	51	51	60	60	58
As	11.30	6.50	11.20	8.50	9.20	6.20	1.29	2.20	1.70
Br	8.70	10.40	13.00	3.33	17.20	15.40	33.90	16.90	8.40
Rb	35	20	35	27	29	21	7	11	9
Sb	0.93	0.54	0.99	0.76	0.95	0.75	0.10	0.20	0.20
Cs	1.42	0.81	1.44	1.01	1.24	0.83	0.38	0.37	0.34
Ba	511	346	547	454	503	392	99	255	267
La	10.08	7.09	8.91	8.83	7.40	5.77	3.56	4.45	4.46
Ce	22.80	16.90	18.70	18.80	14.80	12.80	9.70	11.00	11.00
Nd	8.8	8.6	7.1	9.5	6.4	6.6	8	7.7	8
Sm	2.60	2.76	2.03	2.57	1.90	2.00	2.41	2.40	2.34
Eu	0.69	0.84	0.57	0.75	0.62	0.66	0.89	0.82	0.81
Tb	0.35	0.42	0.28	0.34	0.28	0.29	0.50	0.39	0.35
Yb	1.12	1.28	0.96	1.09	0.97	0.91	1.84	1.19	1.17
Lu	0.17	0.179	0.141	0.171	0.138	0.13	0.266	0.184	0.179
Hf	3.75	2.95	3.67	3.36	3.69	3.11	1.74	1.87	1.91
Ta	0.19	0.15	0.19	0.17	0.19	0.17	0.10	0.10	0.09
W	0.2	0	0.2	1	0.5	0.3	0.3	0	0
Th	1.75	1.11	1.73	1.33	1.55	0.97	0.44	0.35	0.39
U	1.20	0.67	0.96	0.80	1.15	0.62	0.34	0.28	0.30

(Continued)

Table 9. (Continued).

Sample	Location										Mean			
	Bering Island													
<i>N</i>	93K63/5	93K63/7	93K63/8	93K63/9	93K63/10	2	6	1	3	8,11,10	<i>n</i> = 3			
SiO ₂	74.50	0.09	72.78	0.63	77.65	0.15	75.86	0.39	75.54	76.62	77.22	79.07	79.30	0.20
TiO ₂	0.36	0.03	0.45	0.03	0.20	0.03	0.36	0.03	0.27	0.20	0.23	0.30	0.26	0.01
Al ₂ O ₃	14.13	0.12	14.49	0.07	12.66	0.09	12.82	0.13	13.73	13.78	13.91	13.23	14.19	0.14
FeO*	2.32	0.05	3.69	0.25	1.40	0.04	1.73	0.10	2.02	1.20	1.33	0.97	1.33	0.05
MnO	0.06	0.04	0.14	0.05	0.05	0.04	0.04	0.04	0.00	0.00	0.01	0.00	0.04	0.05
MgO	0.62	0.02	0.61	0.08	0.21	0.03	0.29	0.04	1.27	0.25	0.40	0.19	0.29	0.02
CaO	2.92	0.07	2.74	0.25	1.37	0.05	1.35	0.07	1.95	1.19	1.37	0.82	1.30	0.05
Na ₂ O	3.28		3.48		4.07		4.17		2.46	3.72	2.29	2.52	1.63	0.11
K ₂ O	1.45	0.03	1.33	0.08	2.12	0.05	3.06	0.05	2.48	2.79	2.90	2.63	1.37	0.19
P ₂ O ₅	0.06	0.03	0.10	0.03	0.02	0.02	0.04	0.02	0.05	0.01	0.02	0.04	0.10	0.09
SO ₂	0.02	0.01	0.02	0.01	0.00	0.00	0.01	0.01	0.02	0.01	0.01	0.00	0.16	0.00
F	0.13	0.07	0.04	0.06	0.11	0.15	0.09	0.11	0.09	0.12	0.10	0.06	0.02	0.02
Cl	0.14	0.03	0.14	0.02	0.14	0.02	0.18	0.03	0.11	0.11	0.19	0.15	0.01	0.01
Total	100.00		100.00		100.00		100.00		100.00	100.00	100.00	100.00	100.00	0.01

Table 9. (Continued).

Location	Bering Island							Mean
	93K63/5	93K63/7	93K63/8	93K63/9	93K63/10	93-K63/6 (mixed)	3	
Sample	7	5	21	7	2	1	3	8,11,10
<i>N</i>	7	5	21	7	2	1	3	<i>n</i> = 3
Bulk analyses								
INa ₂ O	3.40	4.19	3.46	4.01	4.37			4.37
Sc	8.67	17.26	19.38	8.08	12.97			12.97
Cr	5.5	8.1	8.5	4.7	89.8			89.8
IFeO	2.12	3.58	4.30	1.80	3.43			3.43
Co	5.16	6.63	12.94	3.65	18.16			18.16
Zn	43	100	75	43	64			64
As	5.59	4.50	4.20	3.80	7.30			7.30
Br	24.30	22.10	6.40	7.50	10.40			10.40
Rb	11	0	7	36	22			22
Sb	0.45	0.42	0.69	0.46	0.63			0.63
Cs	0.88	0.60	0.63	1.51	0.62			0.62
Ba	324	222	275	530	422			422
La	5.99	5.08	5.85	11.99	6.69			6.69
Ce	14.70	13.30	14.90	28.00	13.40			13.40
Nd	7.7	10.4	9.1	11.6	7.3			7.3
Sm	2.51	3.10	3.01	3.57	1.93			1.93
Eu	0.79	1.09	0.98	0.76	0.99			0.99
Tb	0.45	0.63	0.54	0.57	0.38			0.38
Yb	1.92	2.71	2.21	2.66	1.11			1.11
Lu	0.286	0.396	0.348	0.416	0.162			0.162
Hf	3.26	2.96	2.61	5.67	2.80			2.80
Ta	0.13	0.38	0.10	0.32	0.10			0.10
W	0	0	0.7	0.6	0			0
Th	0.87	0.81	0.62	2.59	0.74			0.74
U	0.44	0.39	0.30	1.58	0.70			0.70

N, number of analyses averaged.
^aNa₂O values normalized (see text).

Table 10. Microprobe analyses of glass from tephra samples from Attu Island.

Sample	95-01/1	95-01/2	95-02/1	95-06/1				
N	8	9	6	8				
SiO ₂	75.25	0.19	75.30	0.19	74.44	0.37	75.73	0.14
TiO ₂	0.29	0.03	0.27	0.04	0.30	0.03	0.30	0.03
Al ₂ O ₃	14.33	0.14	14.16	0.17	14.56	0.14	13.97	0.16
FeO	1.37	0.04	1.37	0.05	2.08	0.10	1.40	0.07
MnO	0.02	0.03	0.06	0.05	0.08	0.06	0.02	0.02
MgO	0.35	0.06	0.32	0.04	0.45	0.05	0.35	0.02
CaO	1.34	0.06	1.33	0.04	2.18	0.13	1.38	0.04
Na ₂ O ^a	4.11		4.36		3.78		3.90	
K ₂ O	2.63	0.07	2.58	0.08	1.86	0.06	2.70	0.09
P ₂ O ₅	0.06	0.03	0.05	0.02	0.06	0.02	0.06	0.02
SO ₂	0.02	0.01	0.03	0.01	0.01	0.01	0.04	0.02
F	0.06	0.09	0.01	0.02	0.05	0.07	0.01	0.03
Cl	0.16	0.06	0.16	0.05	0.14	0.05	0.14	0.03
Total	100.00		100.00		100.00		100.00	

Sample	95-01/3 (mixed)											
	4	16	3	10	9	11	14	15	8	5	12	1
SiO ₂	68.47	69.96	70.52	71.61	71.73	73.00	74.95	75.24	75.55	75.88	75.97	76.29
TiO ₂	0.65	0.69	0.74	0.73	0.63	0.50	0.27	0.35	0.31	0.28	0.26	0.24
Al ₂ O ₃	15.89	15.54	15.42	14.76	15.17	14.83	14.64	14.33	14.44	14.24	14.11	14.06
FeO	4.27	3.89	3.78	3.75	3.47	2.87	1.92	1.93	1.84	1.75	1.82	1.76
MnO	0.00	0.05	0.11	0.04	0.08	0.00	0.07	0.07	0.02	0.00	0.04	0.07
MgO	1.25	1.09	0.98	0.93	0.81	0.76	0.44	0.45	0.48	0.35	0.40	0.32
CaO	3.66	3.22	3.26	3.14	2.95	2.68	2.08	2.06	2.05	1.87	1.85	1.81
Na ₂ O ^a	3.87	3.46	3.17	2.99	3.27	3.33	3.52	3.48	3.16	3.59	3.47	3.43
K ₂ O	1.54	1.64	1.70	1.65	1.63	1.81	1.89	1.90	1.88	1.84	1.91	1.80
P ₂ O ₅	0.18	0.19	0.15	0.20	0.13	0.08	0.08	0.06	0.08	0.00	0.02	0.02
SO ₂	0.03	0.00	0.00	0.01	0.02	0.00	0.00	0.01	0.02	0.01	0.00	0.00
F	0.08	0.12	0.07	0.00	0.00	0.02	0.02	0.00	0.06	0.06	0.00	0.07
Cl	0.11	0.16	0.10	0.18	0.11	0.11	0.11	0.13	0.11	0.11	0.14	0.14
Total	100.00	100.00	100.00	100.00	100.00	100.00	100.00	100.00	100.00	100.00	100.00	100.00

N, number of analyses averaged;
^aNa₂O values were normalized (see text).

Peat sections on Bering Island, Commander Islands

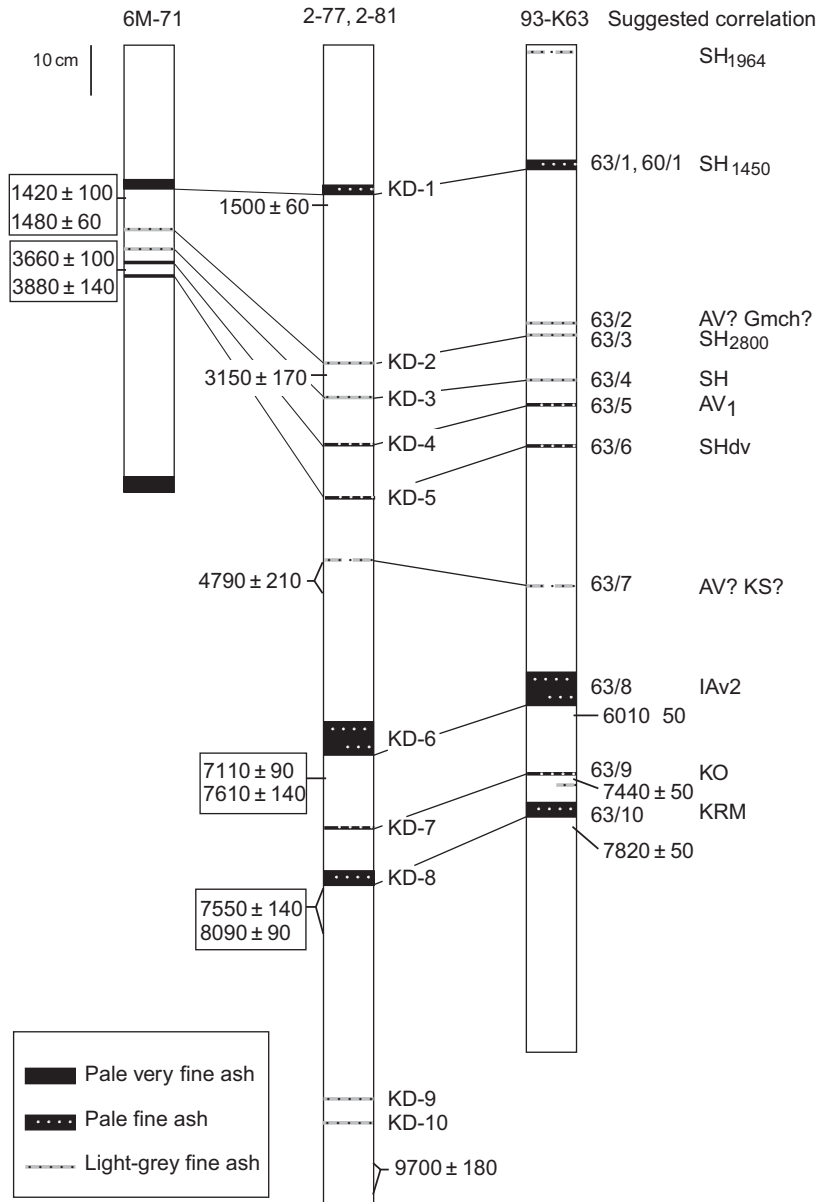


Figure 9. Peat sections on Bering Island measured and sampled by different researchers. Sections 6M-71, 2-77, and 2-81 according to Kirianov *et al.* (1990). Section 93-K63 measured and sampled by I.V. Melekestsev (unpublished data) is located in the northern part of the island. Sample IDs are shown to the right of the sections. Radiocarbon dates were obtained on bulk peat samples. Dates in boxes were obtained on successive alkaline extractions from the same sample. Codes of suggested correlatives are as in Table S1; Gmch is a code for Gamchen volcano.

younger than AV₁. Another eruptive source may be Barany Cone at Gamchen volcano, which started to form ~3600 ¹⁴C year BP and also erupted low-K basaltic andesite (Ponomareva *et al.* 2007a), but there is a lack of glass analyses from the Barany Cone eruptions and hence we prefer an unknown Avachinsky eruption.

Tephra layers 93K63/3 (KD-2) and 93K63/4 (KD-3)

Tephra layer 93K63/3 is younger than 3150 ± 170 ¹⁴C year (Figure 9), whereas layer 93K63/4 is between 3150 ± 170 and 3660 ± 100 ¹⁴C year (Kirianov *et al.* 1990). The K₂O, FeO, and CaO contents of the glasses are typical of Shiveluch tephra (Figure 7). Bulk samples of the tephra have high Cr contents also typical of Shiveluch (Table 7) tephra. We therefore correlate both tephra with eruptions from Shiveluch. The SH₁, SH₃, and SH₁₄₅₀ eruptions all occurred >1500 years prior to the deposition of the 93K63/3 and 93K63/4 tephra. Isopachs for the SH₂₈₀₀ eruption (Figure 2G) extend towards Bering Island, and it is probable that this was the source of the younger 93K63/3 tephra. The older tephra must be from Shiveluch, but we cannot identify a specific eruption at this time.

Tephra layer 93K63/5 (KD-4)

This tephra is dated at ~3500 ¹⁴C year BP (Kirianov *et al.* 1990). The glass is homogeneous and has a low K₂O content of 1.45 wt.% and CaO and FeO contents consistent with an eruption from either Avachinsky or Ksudach (Figure 7). The bulk trace element analyses for some elements are compositionally similar to KS and AV tephra, although the La/Yb is distinctly higher than KS and typical of AV tephra (Figure 8). The AV₁ eruption has a radiocarbon age of 3500 years, but our samples from close to the source (<10 km from vent) show it was very heterogeneous in composition (Table 4). There are general similarities in the average glass composition of tephra 93K63/5 with some individual glass analyses from AV₁ tephra (Table 4). We consider the AV₁ eruption that had a NE dispersal axis (Figure 4B) to be the prime candidate, but in more distal locations, if our correlation is correct, the AV₁ tephra was homogeneous and rhyolitic in composition.

Tephra layer 93K63/6 (KD-5)

This tephra was dated at ~4000 ¹⁴C year BP by Kirianov *et al.* (1990) who suggested that it was erupted from the Shiveluch volcano. Microprobe analyses of the glass show a mixed population of compositions (Table 9). The K₂O contents of four shards range from 2.5 to 2.9 wt.% K₂O consistent with Shiveluch (Table 7). The INAA of the bulk sample has a Cr content of 90 ppm also consistent with Shiveluch (Figure 8) as the source. The tephra is correlated with the SH_{dv} eruption at 4100 ¹⁴C year BP; although the dispersal axis for this eruption was more to the NE, it is still probably to be the best relative (Figure 2).

Tephra layer 93K63/7

This tephra was dated at ~4800 ¹⁴C year BP (Kirianov *et al.* 1990). The glass has a low K₂O content of 1.33 wt.% that puts it in the field of AV or KS eruptions. The FeO content of the glass (Table 9) is more similar to that of KS glasses (Table 7). The INAA shows an La/Yb <2 and it plots in the KS field on the Th versus La/Yb variation diagram (Figure 8), but it plots not far from the field for AV tephra. The KS₂ eruption was ~6000 ¹⁴C year BP, 1200 years prior to the deposition of the 93K63/7 tephra; hence, unless the age of the

tephra is incorrect, the KS₂ eruption is an unlikely correlative. The Avachinsky IAv20 (AV₃) eruption was ~4500 ¹⁴C year BP and produced a tephra volume of 1.1 km³ with a dispersal axis directed to the E (Braitseva *et al.* 1998). Overall, the geochemical data are more consistent with this being a KS tephra, but an AV source cannot be discounted.

Tephra layer 93K63/8 (KD-6)

This tephra has an age of ~7000 ¹⁴C year BP and is the thickest (7 cm) in the peat section (Kirianov *et al.* 1990). Kirianov *et al.* (1990) suggested that the tephra was erupted from the Shiveluch volcano. INAAs of a bulk sample show that it has a low Cr content inconsistent with Shiveluch as a source. The La/Yb ratio falls in the AV field in Figure 8. The IAv2 eruption from Avachinsky has a radiocarbon age of 7150 year BP and produced >8–10 km³ of tephra. The dispersal axis was towards the Bering Island (Braitseva *et al.* 1998). We conclude that this tephra layer correlates with the IAv2 Avachinsky eruption.

Tephra layer 93K63/9 (KD-7)

This tephra has an age of ~7500 ¹⁴C year BP based on dates of the enclosing peat (Kirianov *et al.* 1990). Kirianov *et al.* (1990) correlated the tephra with the KZ eruption (7500 ¹⁴C year BP) based on the refractive index of the glass, the mineralogy, and age. On the basis of the age, the most likely correlatives for this tephra are the KZ or KO eruptions. Glass from the tephra has 2.12 wt.% K₂O (Table 9), which is nearly identical to that of KO glasses (2.09 wt.% K₂O) and significantly different from that of KZ glasses (3.04 wt.% K₂O) (Table 2). The bulk INAA of the tephra shows it to fall in the range of Th content and La/Yb ratio of the KO eruption from the Kurile Lake. KZ tephra have a much higher La/Yb significantly different to that of the 93K63/9 tephra. The geochemical data show conclusively that the tephra correlates with the KO eruption.

The occurrence of KO tephra on the Bering Island is significant because isopachs and field studies have suggested that the eruption dispersal axis was to the NE and not to the NW (Figure 3A). To date, the northernmost site in eastern Kamchatka where the KO has been identified earlier is Maly Semiachik volcano (Braitseva *et al.* 1995). Ignimbrites from the KO eruption entered the sea on the E side of the Kamchatka Peninsula and could have produced a secondary co-ignimbrite eruption cloud that was dispersed in the direction of the Bering Islands without leaving a significant marker on the mainland.

Tephra layer 93K63/10 (KD-8)

This tephra has an age of ~7800 ¹⁴C year BP based on dates of a peat layer below the tephra layer (Figure 9). Kirianov *et al.* (1990) suggested that the tephra was from the 7900 ¹⁴C year BP KRM eruption based on age and the mineral composition of the tephra. The glass K₂O content of 3.06 wt.% (Table 9) is identical to that of the KRM tephra (3.01 wt.% K₂O content) (Table 1, Figure 7). The La/Yb ratio of 4.5 for a bulk sample of the tephra is identical to that of the KRM tephra (Figure 8). We conclude that this tephra correlates with the KRM eruption from Karymsky.

Karaginsky Island and Uka Bay samples

Two samples (93K38/1 and 93K30/1) from Karaginsky Island and one (93K50/1) from Uka Bay were collected from the very top of separate sections and were correlated in the

field based on their appearance and stratigraphy (Melekestsev and Kurbatov 1998). A radiocarbon age of 160 ± 40 ^{14}C year BP was obtained below sample 93K50/1 from Uka Bay. Sample 93K30/2 from Karaginsky Island was lower in the section and beneath the other two Karaginsky Island samples.

Glass compositions from all four glasses show a very limited range of K_2O contents (2.71–2.81 wt.%) (Table 9), consistent with eruption from Shiveluch volcano (Table 7). Bulk analyses of the four tephra all have Cr contents >98 ppm characteristic of SH tephra samples and plot in the middle of the SH field on the Cr versus Th plot (Figure 8). The four tephra were clearly erupted from Shiveluch.

Based on their inferred age and suggested correlation with each other, the three samples (93K38/1, 93K30/1, and 93K50/1) are correlated with the 1854 Shiveluch eruption. Sample 93K30/2 from Karaginsky Island is lower in the section, and the glass and bulk compositions show that it was erupted from Shiveluch. With no radiocarbon dates to constrain its age, the 93K30/2 tephra cannot be correlated with any specific Shiveluch eruption.

Attu Island tephra

Five tephra collected on Attu Island in the Aleutians (Figure 1) were analysed for major elements by EMP (Table 10). Samples and their preliminary radiocarbon ages were provided by Tom Miller (1995, personal communication). The radiocarbon ages and field data suggest all the tephra were erupted between 3000 and 5100 years ago.

Four of the tephra have homogeneous rhyolitic glass compositions, and one tephra is mixed with glasses ranging from dacite to rhyolite (Figures 6 and 7). The tephra are most likely the products of Kamchatka volcanism based on the prevailing wind direction that is from W to E. Explosive Holocene eruptions in Kamchatka occurring in this time period with dispersal axes directed eastward include SH, Op_{tr} , and AV eruptions.

Tephra samples 95-01/1, 95-01/2, and 95-06/1 have K_2O contents ranging from 2.6 to 2.7 wt.% that are typical of SH tephra (Table 7). The FeO (1.37–1.40 wt.%) and CaO (1.33–1.38) contents (Table 10) of the glasses are also typical of Shiveluch glasses (Table 7). We conclude that the three tephra are from Shiveluch, but because of the uncertainty in their ages, we cannot correlate the tephra with any specific eruption. There are numerous large SH eruptions between 2800 and 5600 ^{14}C year BP (Ponomareva *et al.* 2007b).

The mixed tephra 95-01/3 is more difficult to identify. It is clearly of the low K_2O type. We tentatively suggest that it may be an AV tephra based on the overlap of chemical compositions with the AV_1 tephra as shown in Figure 7. The age for the tephra, which is between 4200 and 5100 ^{14}C year BP, precludes it from being AV_1 , but the tephra clearly show geochemical characteristics of AV tephra.

Tephra 95-02/1 is homogeneous, and the composition is similar to some of the glass shards in the mixed tephra 95-01/3 (Table 10). It is also of the low K_2O variety. The tephra has a glass composition that shows the greatest similarity to AV tephra.

Conclusions

Twenty-seven key-marker tephra layers erupted from 11 volcanic centres in Kamchatka were chemically characterized on the basis of major element compositions of volcanic glass. This is the first systematic attempt to ‘chemically fingerprint’ the major Holocene tephra in Kamchatka using glass compositions. Most of the glasses have homogeneous compositions, although two have mixed compositions probably as a result of being

erupted from zoned magma chambers. Two tephra had multimodal glass compositions. The glass from 21 of the tephra is rhyolitic and two are dacitic. Many of the tephra resulted from eruptions that had andesite or dacite bulk compositions. As this was a pilot study and was based on 89 samples, no attempt has been made to apply statistical techniques to differentiate the glasses. The difference can be clearly seen on simply major element variation diagrams and suggests that statistical analysis, especially on a bigger sample population, could prove very useful. K_2O contents of the glasses in combination with CaO , FeO , and Al_2O_3 are sufficient to identify the eruptive centre for many tephra.

Sixty-four bulk ash samples were analysed by INAA to further refine the geochemical characteristics of Kamchatka tephra. This simple approach saved the need to do glass separates and proved very useful. Tephra from 10 eruptive centres can be characterized on the basis of Cr and Th contents and La/Yb ratios. This pilot study illustrates that significant trace element variations exist, and future studies using the new laser ablation ICP-MS analytical techniques could prove very useful.

We have illustrated the usefulness of using the geochemical features in combination with field relationships and radiocarbon ages and identified the eruptive centres for tephra on Bering Island and Attu Island, which is in the Aleutian Island arc over 500 km W of the Kamchatka Peninsula.

Acknowledgements

Research described in this article was supported in part by the grants 09-05-00286 and 09-05-00718 from the Russian Foundation for Basic Research. Most of the analysed tephra samples were collected, thanks to field grants from the National Geographic Society to VP. We cordially thank Olga Braitseva, Lilia Bazanova, Maria Pevzner, Ivan Melekestsev, Andrei Kurbatov, Oleg Dirksen, and Tom Miller for additional samples. Financial support from NSF grant #EAR-0125787 to Joanne Bourgeois has allowed VP to accomplish her work on the manuscript. We greatly appreciate the help of Dr Nelia Dunbar and her staff and student workers at the Electron Microprobe Lab at N.M. Tech for assistance. Most of analyses reported here were made by RRS as part of her MS thesis studies. PK acknowledges the support from the Office of Polar Programs, NSF.

References

- Alloway, B.V., Larsen, G., Lowe, D.J., Shane, P.A.R., and Westgate, J.A., 2007, Tephrochronology, *in* Elias, S.A., ed., *Encyclopedia of quaternary science*: London, Elsevier, p. 2869–2898.
- Andrews, B.J., Gardner, J.E., Tait, S., Ponomareva, V., and Melekestsev, I.V., 2007, Dynamics of the 1800 ^{14}C yr BP caldera-forming eruption of Ksudach volcano, Kamchatka, Russia, *in* Eichelberger, J., Gordeev, E., Kasahara, M., Izbekov, P., and Lees, J., eds., *Volcanism and subduction: The Kamchatka region*. Geophysical Monograph Series: Washington DC, American Geophysical Union, v. 172, p. 325–342.
- Bazanova, L.I., Braitseva, O.A., Dirksen, O.V., Sulerzhitsky, L.D., and Danhara, T., 2005, Ashfalls from the largest Holocene eruptions along the Ust'-Bol'sheretsk – Petropavlovsk-Kamchatsky traverse: sources, chronology, recurrence: *Volcanology and Seismology*, v. 6, p. 30–46 (In Russian).
- Bazanova, L.I., Braitseva, O.A., Melekestsev, I.V., and Sulerzhitsky, L.D., 2004, Catastrophic eruptions of Avachinsky volcano (Kamchatka) in Holocene: chronology, dynamics, geological effect, environmental impact and long-term forecast: *Volcanology and Seismology*, v. 6, p. 15–20 (In Russian).
- Bazanova, L.I., Braitseva, O.A., Puzankov, M.Yu., and Sulerzhitsky, L.D., 2003, Catastrophic plinian eruptions of the initial cone-building stage of the Young Cone of Avachinsky volcano (Kamchatka): *Volcanology and Seismology*, v. 6, p. 20–40 (In Russian).
- Bazanova, L.I., and Pevzner, M.M., 2001, Khangar: One more active volcano in Kamchatka: Transactions (Doklady) of the Russian Academy of Sciences, Earth Sciences, v. 377A, p. 307–310.
- Braitseva, O.A., Bazanova, L.I., Melekestsev, I.V., and Sulerzhitsky, L.D., 1998, Largest Holocene eruptions of Avachinsky volcano, Kamchatka: *Volcanology and Seismology*, v. 20, p. 1–27.

- Braitseva, O.A., Melekestsev, I.V., Ponomareva, V.V., and Kirianov, V.Yu., 1996, The caldera-forming eruption of Ksudach volcano about cal. AD 240, the greatest explosive event of our era in Kamchatka: *Journal of Volcanology and Geothermal Research*, v. 70, p. 49–66.
- Braitseva, O.A., Melekestsev, I.V., Ponomareva, V.V., and Sulerzhitsky, L.D., 1995, Ages of calderas, large explosive craters and active volcanoes in the Kuril-Kamchatka region, Russia: *Bulletin of Volcanology*, v. 57, p. 383–402.
- Braitseva, O.A., Ponomareva, V.V., Sulerzhitsky, L.D., Melekestsev, I.V., and Bailey, J., 1997, Holocene key-marker tephra layers in Kamchatka, Russia: *Quaternary Research*, v. 47, p. 125–139.
- Dirksen, O.V., Ponomareva, V.V., and Sulerzhitsky, L.D., 2002, Eruption from Chasha Crater – a unique large silicic eruption at a monogenetic basaltic lava field: *Volcanology and Seismology*, v. 5, p. 3–10 (In Russian).
- Hallett, R.B., and Kyle, P.R., 1993, XRF and INAA determinations of major and trace elements in Geological Survey of Japan igneous and sedimentary rock standards: *Geostandards Newsletter*, v. 17, p. 127–133.
- Hunt, J.B., and Hill, P.G., 1993, Tephra geochemistry: a discussion of some persistent analytical problems: *The Holocene*, v. 3, p. 271–278.
- Keller, J., 1981, Quaternary tephrochronology in the Mediterranean, in Self, S., and Sparks, R.S.J., eds., *Tephra studies: Dordrecht, Reidel*, p. 227–244.
- Kirianov, V.Yu., Egorova, I.A., and Litasova, S.N., 1990, Volcanic ash on Bering Island (Commander Islands) and Kamchatkan Holocene eruptions: *Volcanology and Seismology*, v. 8, p. 850–868.
- Knox, R.W.O'B., 1993, Tephra layers as precise chronostratigraphical markers, in Hailwood, E.A., and Kidd, R.B., eds., *High resolution stratigraphy: Geological Society Special Publication*, v. 70, p. 169–186.
- Korotev, R.L., 1987, National Bureau of Standards coal flyash (SRM 1633a) as a multielement standard for instrumental neutron activation analysis: *Journal of Radioanalytical and Nuclear Chemistry*, v. 110, p. 159–177.
- Le Bas, M.J., Le Maitre, R.W., Streckeisen, A., and Zanettin, B., 1986, A chemical classification of volcanic rocks based on the total alkali–silica diagram: *Journal of Petrology*, v. 27, p. 745–750.
- Lindstrom, D.J., and Korotev, R.L., 1982, TEABAGS: Computer programs for instrumental neutron activation analysis: *Journal of Radioanalytical and Nuclear Chemistry*, v. 70, p. 439–458.
- Melekestsev, I.V., Braitseva, O.A., Bazanova, L.I., Ponomareva, V.V., and Sulerzhitsky, L.D., 1996a, A particular type of catastrophic explosive eruptions with reference to the Holocene sub-caldera eruptions at Khangar, Khodutka Maar, and Baraniy Amfiteatr volcanoes in Kamchatka: *Volcanology and Seismology*, v. 18, p. 135–160.
- Melekestsev, I.V., Braitseva, O.A., Erlich, E.N., and Kozhemyaka, N.N., 1974, Volcanic mountains and plains, in Luchitsky, I.V., ed., *Kamchatka, Kurile and Commander Islands Nauka, Moscow*, p. 162–234.
- Melekestsev, I.V., Braitseva, O.A., Ponomareva, V.V., and Sulerzhitsky, L.D., 1996b, Holocene catastrophic caldera-forming eruptions of Ksudach volcano, Kamchatka: *Volcanology and Seismology*, v. 17, p. 395–421.
- Melekestsev, I.V., and Kurbatov, A.V., 1998, Frequency of large paleoearthquakes at the northwestern coast of the Bering Sea and in the Kamchatka Basin during late Pleistocene/Holocene time: *Volcanology and Seismology*, v. 19, p. 257–267.
- Melekestsev, I.V., Litasova, S.N., and Sulerzhitsky, L.D., 1992, On the age and scale of the directed-blast catastrophic eruption of the Avachinsky volcano (Kamchatka) in the Late Pleistocene: *Volcanology and Seismology*, v. 13, p. 135–146.
- Melekestsev, I.V., Ponomareva, V.V., and Volynets, O.N., 1995, Kizimen volcano (Kamchatka) – future Mt. St. Helens?: *Journal of Volcanology and Geothermal Research*, v. 65, p. 205–226.
- Neilson, C.H., and Sigurdsson, H., 1981, Quantitative methods for electron microprobe analysis of sodium in natural and synthetic Glasses: *American Mineralogist*, v. 66, p. 547–552.
- Pevzner, M.M., Ponomareva, V.V., and Melekestsev, I.V., 1998, Chernyi Yar reference section of Holocene ash markers at the northeastern coast of Kamchatka: *Volcanology and Seismology*, v. 19, p. 389–406.
- Ponomareva, V.V., Kyle, P.R., Melekestsev, I.V., Rinkleff, P.G., Dirksen, O.V., Sulerzhitsky, L.D., Zaretskaia, N.E., and Rourke, R., 2004, The 7600 (¹⁴C) year BP Kurile Lake caldera-forming eruption, Kamchatka, Russia: Stratigraphy and field relationships: *Journal of Volcanology and Geothermal Research*, v. 136, p. 199–222.

- Ponomareva, V.V., Kyle, P.R., Pevzner, M., Sulerzhitsky, L., and Hartman, M., 2007b, Holocene eruptive history of Shiveluch volcano, Kamchatka Peninsula, Russia, *in* Eichelberger, J., Gordeev, E., Kasahara, M., Izbekov, P., Lees, J., eds., *Volcanism and subduction: The Kamchatka region*. Geophysical Monograph Series: Washington DC, American Geophysical Union, v. 172, p. 263–282.
- Ponomareva, V.V., Melekestsev, I., Braitseva, O., Churikova, T., Pevzner, M., and Sulerzhitsky, L., 2007a, Late Pleistocene-Holocene volcanism on the Kamchatka Peninsula, northwest Pacific region, *in* Eichelberger, J., Gordeev, E., Kasahara, M., Izbekov, P., and Lees, J., eds., *Volcanism and subduction: The Kamchatka region*. Geophysical Monograph Series: Washington DC, American Geophysical Union, v. 172, p. 263–282.
- Shane, P., 2000, Tephrochronology: a New Zealand case study: *Earth-Science Reviews*, v. 49, p. 223–259.
- Volynets, O.N., 1994, Geochemical types, petrology and genesis of Late Cenozoic volcanic rocks from the Kurile-Kamchatka island-arc system: *International Geology Review*, v. 36, p. 373–405.
- Volynets, O.N., Ponomareva, V.V., Braitseva, O.A., Melekestsev, I.V., and Chen, Ch.H., 1999, Holocene eruptive history of Ksudach volcanic massif, South Kamchatka: evolution of a large magmatic chamber: *Journal of Volcanology and Geothermal Research*, v. 91, p. 23–42.
- Zaretskaya, N.E., Ponomareva, V.V., and Sulerzhitsky, L.D., 2007, Radiocarbon dating of large Holocene volcanic events within South Kamchatka (Russian Far East): *Radiocarbon*, v. 49, p. 1065–1078.